Endogenous corazonin signaling modulates the post-mating switch in behavior and physiology in females of the brown planthopper and *Drosophila*

Ning Zhang (张宁)[1], Shao-Cong Su (苏少聪)[1], Ruo-Tong Bu (卜若彤)[1], Yi-Jie Zhang (张伊杰)[1], Lei Yang (杨磊)[1], Jie Chen (陈洁)[1], Dick R. Nässel[2], Cong-Fen Gao (高聪芬)[1], Shun-Fan Wu (吴顺凡)[1*]

Orcid ID numbers of Shun-Fan Wu: 0000-0003-0096-147X

Orcid ID numbers of Dick Nässel: 0000-0002-1147-7766

Affiliations:

[1]State Key Laboratory of Agricultural and Forestry Biosecurity, College of Plant Protection, Nanjing Agricultural University, Nanjing 210095, China

[2]Department of Zoology, Stockholm University, Stockholm, Sweden

[*]Correspondence: wusf@njau.edu.cn (S.F. Wu).

Abstract

Mating in insects typically triggers a post-mating response (PMR) in females, characterized by reduced receptivity to re-mating and increased oviposition, which ensures numerous and viable offspring and male paternity. This PMR is induced by male seminal factors, such as sex peptide in *Drosophila melanogaster*, as well as intrinsic female signaling components. The latter signaling remains poorly understood in most insects, including the devastating rice pest, the brown planthopper (BPH) *Nilaparvata lugens*. Here, we show that the neuropeptide corazonin (CRZ) and its receptor (CrzR) are critical for the PMR in female BPHs. Peptide injection, RNAi knockdown, and CRISPR/Cas9 mutagenesis confirm that intact CRZ signaling reduces re-mating frequency and increases ovulation in mated BPH females. The CrzR is highly expressed in the female reproductive tract, and CrzR knockdown phenocopies CRZ diminishment. Importantly, female CRZ/CrzR signaling is required for male seminal factors, such as the peptide maccessin, to induce the PMR; with disrupted *CrzR* signaling, injection of seminal fluid or maccessin fails to reduce female receptivity. Notably, CRZ is not produced in male accessory glands (MAGs) of BPHs and thus not transferred during copulation. We furthermore demonstrate that also in *D. melanogaster* disrupted CRZ signaling increases female re-mating and reduces oviposition, while CRZ injection suppresses virgin receptivity and increases oviposition. Finally, we detected no CRZ in the MAG of *D. melanogaster,* supporting its role as an endogenous signal in the female PMR also in this species. In summary, our findings reveal a conserved role of endogenous CRZ signaling in regulating the female PMR and demonstrate that female CRZ signaling and male-derived signals cooperate to induce post-mating transitions in BPHs and *D. melanogaster*. CRZ is a paralog of the peptide gonadotropin-releasing hormone, known to regulate reproduction in vertebrates, including humans, suggesting evolutionary conservation of an ancient function.

Keywords: Post mating response; *Nilaparvara lugens*; *Drosophila melanogaster*; corazonin; corazonin receptor

Introduction

Reproductive behavior in animals is influenced by a complex interplay between external sensory inputs and internal states, and is regulated by neuronal and hormonal signaling. In insects, males typically initiate mating through courtship, while females determine acceptance by integrating external sensory cues with their internal state. Consequently, female reproductive activity is modulated by multiple signaling pathways [1-8]. Importantly, in insects, successful copulation commonly induces profound physiological and behavioral changes in the females [5,9-18].

Following their first mating, insect females typically reject further courtship attempts and initiate oviposition. This distinct shift in behavior and physiology is referred to as a post-mating response (PMR) [5-7,19-23]. Induction of a PMR has been documented across diverse insect taxa, for example in *D. melanogaster*, mosquitos *Anopheles gambiae, Aedes aegypti,* crickets (*Gryllodes sigillatus*), and the brown planthopper (BPH), *Nilaparvata lugens* [6,10,15,18,21,24-28].

Induction of a PMR commonly requires the transfer of specific seminal fluid components during copulation. In *D. melanogaster*, seminal fluid peptides, including sex peptide (SP) and DUP99B produced in male accessory glands (MAG), enter the female reproductive tract, bind to specific receptors on sensory neurons, and activate signaling pathways that drive post-mating behavior and physiology [6,13,14,18,29]. Additional factors such as Acp26Ab and ovulin (Acp26Aa) are also transferred with the seminal fluid and modulate female reproductive physiology in *D. melanogaster* [30-33]. Notably, it has been shown that the PMR-inducing substances, produced in the MAG

72 of various insects, are highly species-specific and not even conserved across related
73 taxonomic groups [24,34].

74 While MAG-derived sex peptide (SP) and its receptor (SPR) are key regulators of
75 the female post-mating response (PMR) in *D. melanogaster* [5-7,16], additional signaling
76 pathways intrinsic to females also modulate this process. Interneurons within
77 abdominal neuromeres of the ventral nerve cord (VNC) promote receptivity to males
78 by signaling via myoinhibitory peptide (MIP) to brain circuits [35]. Furthermore, the
79 neuropeptide diuretic hormone 44 (DH44) modulates female sexual receptivity
80 through a sex-specific brain circuit; mating suppresses DH44 signaling, thereby
81 reducing receptivity [1]. During sexual maturation, leucokinin (LK)-expressing neurons
82 (ABLKs) in the abdominal ganglion, downstream of SP-activated circuitry, suppress
83 female receptivity [36]. In addition to changes in receptivity, the *D. melanogaster* PMR
84 includes a shift in diet preference toward yeast consumption. This altered feeding
85 behavior is mediated by specific peptidergic neurons (ALKs) in the brain through LK
86 signaling [12].

87 Although the mechanisms and neuronal pathways underlying the post-mating
88 response (PMR) in *D. melanogaster* are well characterized [3,4,6,7,37-40], this process
89 remains poorly understood in most non-model insects. A prominent example is the
90 brown planthopper (BPH), *N. lugens* (Hemiptera). As a monophagous rice pest, the
91 BPH exhibits robust reproductive capacity and remarkable environmental adaptability
92 [41]. It has also developed high resistance to diverse chemical pesticides [42-44].

93 Consequently, elucidating reproductive physiology and behavior in BPHs is crucial for
94 developing novel control strategies.

95 In BPHs, the recently identified MAG-derived peptide maccessin (macc) is
96 transferred during copulation and triggers a PMR in females, although its receptor
97 remains unknown [24]. Notably, the same study demonstrated that a second peptide,
98 ion transport-like peptide 1 (ITPL-1), also modulates the PMR. Whereas macc is
99 male-specific, ITPL-1 is produced both in the MAG and endogenously in females,
100 where it reduces female receptivity to courting males [24]. Given its endogenous female
101 expression, ITPL-1 likely functions as an intrinsic signaling component in the PMR of
102 BPHs, analogous to the role of myoinhibitory peptide (MIP) and DH44 in *D.*
103 *melanogaster* females [1,35].

104 Here, we explored the role of another neuropeptide, corazonin (CRZ), in the
105 reproductive behavior of BPHs. In *D. melanogaster* males, CRZ is released from
106 interneurons of the ventral nerve cord (VNC) and acts on serotonergic projection
107 neurons to regulate ejaculation and copulation duration [45], mitigates mating-induced
108 heart rate acceleration for physiological recovery [46] and influences post-mating dietary
109 preference [12]. Surprisingly, the role of CRZ signaling in female reproduction remains
110 unexplored. To address this gap, we investigated the role of CRZ in female
111 reproduction, including the PMR, in BPHs and *D. melanogaster.*

112 Here, we demonstrate that CRZ induces a post-mating switch in receptivity in
113 females of both species. CRZ injection in virgin females reduces receptivity to
114 courting males and increases oviposition, while *Crz* knockdown or knockout in mated
115 females restores receptivity to re-mating and decreases oviposition. Notably, CRZ is

116 not produced in the male accessory gland (MAG) of either species and thus the
117 peptide is not transferred during copulation, but acting as an endogenous female
118 peptide signal. In BPHs, the CRZ receptor (CrzR) is highly expressed in the female
119 reproductive tract and both CRISPR-Cas9-mediated *CrzR* knockout and
120 RNAi-mediated knockdown disrupt the PMR, phenocopying CRZ deficiency. Critically,
121 receptivity changes in virgin BPH female, whether induced by MAG extract
122 (containing seminal fluid proteins) or CRZ injection, depend on presence of the CrzR.
123 Collectively, our data demonstrate that endogenous female CRZ signaling and male
124 seminal cues are both required to coordinate post-mating changes in physiology and
125 behavior in females of both insects. CRZ is a paralog of the peptide
126 gonadotropin-releasing hormone, known to regulate reproduction in vertebrates,
127 including humans, suggesting evolutionary conservation of an ancient function.

128

129 # Results

130 ## CRZ signaling reduces receptivity to courting males and stimulates
131 oviposition in *N. lugens* females

132 While numerous studies have established roles of the neuropeptide CRZ in
133 regulating aspects of male reproduction across diverse insect species [47-53], research
134 addressing its potential functions in female reproduction remains conspicuously
135 lacking.

136 This study investigates the role of CRZ in female reproduction, starting with the
137 brown planthopper (BPH), *Nilaparvata lugens*, a major agricultural pest. Initially, the
138 *Crz* gene (GenBank accession: AB817247.1) was cloned based on transcriptome
139 data [54]. The deduced mature CRZ sequence in BPH, pQTFQYSRGWTNamide, is
140 identical to that reported for most studied insect species (Figure 1-figure supplement
141 1A). Consistent with other known CRZ precursors, the BPH precursor encodes a
142 single CRZ peptide starting at the first amino acid of the propeptide (Figure 1-figure
143 supplement 1A and B). A comparison of the organization of selected CRZ precursor
144 genes is shown in Figure 1-figure supplement 1B. Genomic analysis revealed that the
145 CRZ precursor is encoded by two exons separated by a single intron (Figure 1-figure
146 supplement 1B). The mature CRZ peptide and a scrambled control peptide (sCRZ)
147 were synthesized for pharmacological experiments.

148 First, we investigated the role of CRZ signaling in the reproductive behavior and
149 PMR of female BPHs. The PMR in BPHs, is characterized by reduced receptivity to
150 courting males, including display of rejection behaviors, and increased oviposition [24].

151 We found that injection of CRZ significantly reduced receptivity of virgin female BPHs
152 to courting males (Figure 1A and B). Furthermore, virgin females injected with CRZ
153 actively rejected courting males, exhibiting a distinct rejection behavior characterized
154 by ovipositor extrusion and kicking or fleeing. This behavior was not observed in
155 control females injected with sCRZ (Figure 1 Supplementary Video 1). Notably, the
156 CRZ-induced mating refusal behavior in virgin females was no longer observed 24
157 hours after injection (Figure 1-figure supplement 2A). While injection of CRZ peptide
158 did not stimulate egg production in virgin BPHs (Figure 1-figure supplement 2B), it
159 significantly promoted oviposition in mated females (Figure 1C).

160 To further investigate CRZ action, we performed RNA interference (RNAi) by
161 injecting double-stranded *Crz* RNA (*dsNlCrz*) into female BPHs, which efficiently
162 reduced *Crz* expression (Figure 1-figure supplement 2). In *N. lugens*, female
163 receptivity is transiently suppressed after mating and does not begin to recover until at
164 least 72 h after the first mating[24]; therefore, remating assays were performed at 48 h
165 post-mating as shown in Figure 1D. Knockdown of *Crz* resulted in increased
166 receptivity with 10% of the mated females mating again, and significantly reduced
167 oviposition to approximately 60% of control levels (Figure 1E and F). In contrast, *Crz*
168 knockdown had no effect on the receptivity of virgin females (Figure 1E).

169 Since RNAi-mediated knockdown of *Crz* in female BPHs left a residual level of
170 gene expression (Figure 1-figure supplement 2), we generated two *Crz* deletion
171 alleles, ΔCrz^1 and ΔCrz^2, using CRISPR/Cas9 (Figure 1G-G') to achieve a complete
172 ablation. Both alleles harbor deletions eliminating the mature CRZ peptide coding

173 sequence (Figure 1G"). Sanger sequencing confirmed that the deletions
174 compromised essential triplet codons within the *Crz* open reading frame (Figure
175 1-figure supplement 4), thereby efficiently disrupting CRZ peptide expression (Figure
176 1G" and H). Immunohistochemical analysis further validated the mutants, revealing a
177 complete absence of anti-CRZ immunolabeling in homozygous ΔCrz^1 and ΔCrz^2
178 females (Figure 1H). Homozygous ΔCrz^1 and ΔCrz^2 virgin females are fully viable and
179 fertile. They exhibit a courtship vigor similar to controls and their initial mating success
180 rate with wild-type males exceeds 60% (Figure 1I and J). However, 25% of the mated
181 mutant females were receptive to further mating (Figure 1J), and oviposition was
182 significantly reduced to approximately 50% of the wild-type levels (Figure 1K). To
183 further test the *Crz* mutants, we also analyzed mating and oviposition behaviors in *Crz*
184 heterozygous ($+/\Delta Crz^1$) females. Notably, neither the remating rate nor egg
185 production in heterozygous females differed significantly from those of wild-type
186 controls (Figure 1J and K). These results indicate that the *Crz* loss-of-function
187 phenotype is recessive, and that a single functional copy of *Crz* is sufficient to sustain
188 a normal post-mating response (PMR). Collectively, these results demonstrate that
189 diminished CRZ signaling severely perturbs the PMR in female BPHs, seen as
190 increased post-mating receptivity and reduced egg-laying. Importantly, the *Crz*
191 deletion abolished the onset of typical post-mating rejection behavior. We, thus,
192 conclude that endogenous CRZ signaling is important for the induction of a PMR in
193 female BPHs.
194

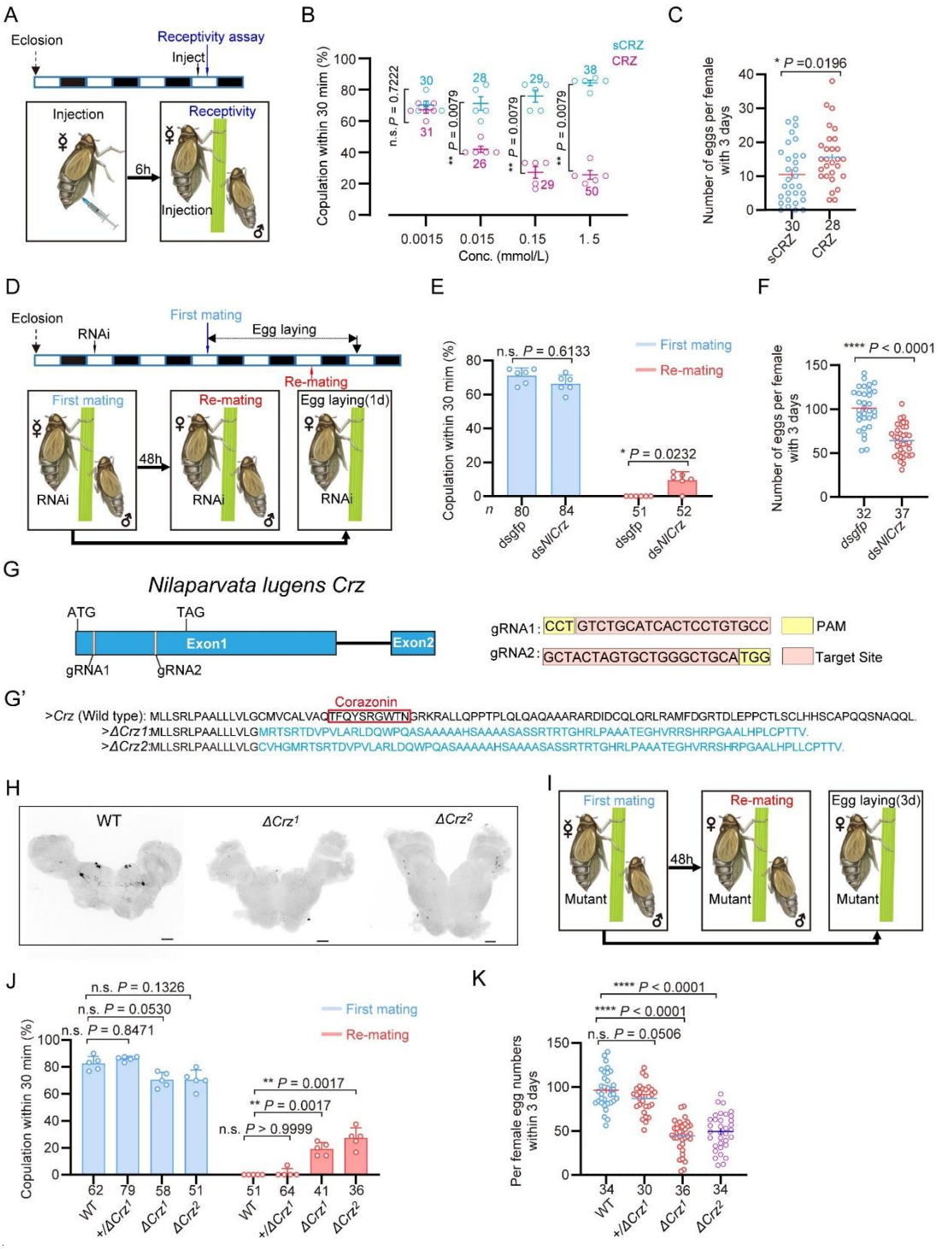

Figure 1. CRZ signaling affects the post-mating response (PMR) and oviposition in female *N. lugens*.

Wild-type males were used in all behavioral assays.

(A) Experimental design for panels B-C. The white/black segments on the experimental time lines denote light/dark periods, respectively.

(B) Receptivity of virgin females 6 h post-injection, using different doses of CRZ (sCRZ as control), each virgin female BPH was injected with a calibrated glass capillary needle directly into the abdomen with 100 ng/10 ng/1 ng/0.1 ng of peptide dissolved in 50 nL of 1 × PBS

204 balanced salt solution. The graph shows percentage females copulating within 30 min. **P <
205 0.01 vs. control; ns (non-significant): P > 0.05 (Mann-Whitney test). The small circles denote
206 the number of replicates, ⩾5 insects/replicate; the numbers above the curves denote total
207 number of animals.
208 (C) Eggs laid per mated female 12 h post-copulation. We used the highest CRZ dose from
209 panel B (sCRZ, control). Each mated female BPH was injected with a calibrated glass capillary
210 needle directly into the abdomen with 100 ng of peptide dissolved in 50 nL of 1 × PBS
211 balanced salt solution. *P < 0.05 (Student's t-test). Data: mean ± s.e.m (⩾4 biological
212 replicates, ⩾6 insects/replicate). The numbers below the bars denote total number of
213 animals.
214 (D) Experimental design for panels E-F.
215 (E) Receptivity of virgin (1st mating) and mated females after *Crz*-RNAi (*dsgfp* as control).
216 Graph displays the percentage of females copulating within 30 min. The small circles denote
217 the number of replicates, ⩾7 insects/replicate; the numbers below the bars denote total
218 number of animals. Statistical comparisons of proportions were performed using chi-square
219 tests for contingency tables, P < 0.05 was considered significant. (F) Total numbers of eggs
220 laid per female over 72 h after *Crz*-RNAi (*dsgfp* as control). ****P < 0.0001 (Student's *t*-test).
221 The small circles and the numbers below the bars denote total number of animals, (⩾4
222 biological replicates, ⩾8 insects/replicate). Data are shown as mean ± s.e.m. (⩾3
223 biological replicates, ⩾8 insects/replicate).
224 (G) Schematic diagram of the *Crz* gene and sgRNA (single-guide RNA) design for *Crz* mutant
225 production. The *Crz* gene consists of 2 exons, and ATG and TAG are located on Exon 1. The
226 target site of the 20 bp sgRNA on Exon 1 is highlighted in pink. The PAM sites are indicated in
227 yellow. The two knockout strains ΔCrz^1 and ΔCrz^2 were unable to produce mature CRZ
228 peptides. (G') The amino acid sequences obtained by translating the mutated base
229 sequences.
230 (H) Absence of CRZ immunoreactivity in homozygous ΔCrz^1 and ΔCrz^2 mutants compared to
231 wild type (WT) expression. Scale bars: 50 μm.
232 (I) Experimental design for panels J-K.
233 (J) Receptivity of virgin/mated females across genotypes. No effect was seen on virgin
234 receptivity, only the re-mating was affected. The small circles denote the number of replicates;
235 ⩾6 insects/replicate, the numbers below the bars denote total number of animals. Statistical
236 comparisons of proportions were performed using chi-square tests for contingency tables, P <
237 0.05 was considered significant.
238 (K) Eggs laid 72 h post-mating. The numbers below the bars denote total number of animals.,
239 ≥4 biological replicates, ≥8 insects/replicate. Data are shown as mean ± s.e.m. ****P < 0.0001;
240 Student's *t* test.

241

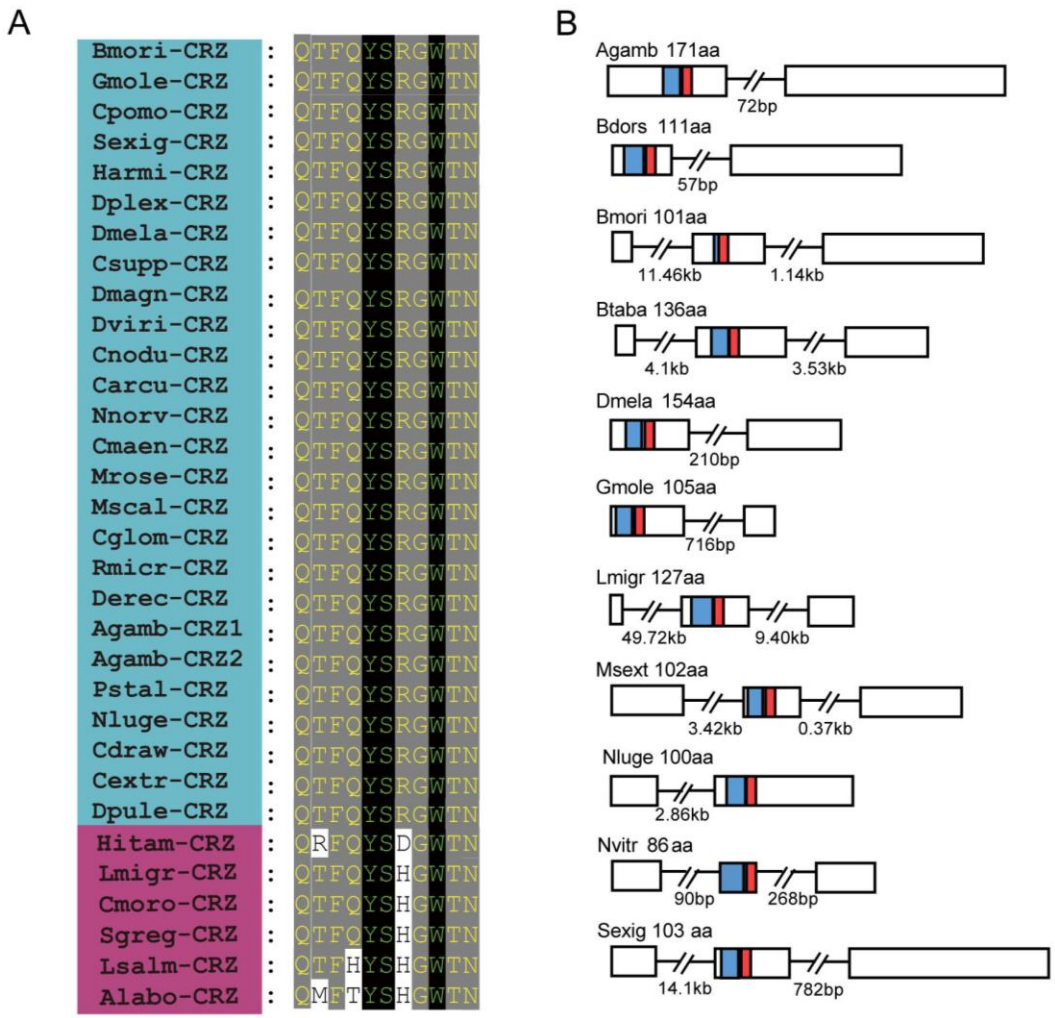

Figure 1 - figure supplement 1. Evolutionary conservation of CRZ peptide sequences in *Nilaparvata lugens* and other arthropods.

(A) Alignment of mature CRZ peptide sequences across species.

Abbreviations of species names are as follows: Bmori (*Bombyx mori*), Gmole (*Grapholita molesta*), Cpomo (*Cydia pomonella*), Sexig (*Spodoptera exigua*), Harmi (*Helicoverpa armigera*), Dplex (*Danaus plexippus*), Dmela (*Drosophila melanogaster*), Csupp (*Chilo suppressalis*), Dmagn (*Daphnia magan*), Dviri (*Drosophila virilis*), Cnodu *(Catagly nodus*), Carcu (*Callinectes arcuatus*), Nnorv (*Nephrops norvegicus*), Cmaen (*Carcinus maenas*), Mrose (*Macrobrachium rosenbergii*), Mscal (*Megaselia scalaris*), Cglom (*Cotesia glomerata*), Rmicr (*Rhipicephalus microplus*), Derec (*Drosophila erecta*), Agamb (*Anopheles gambiae*), Pstal (*Plautia stali*), Nluge (*Nilaparvata lugens*), Cdraw (*Caerostris darwini*), Cextr (*Caerostris extrusa*), Dpule (*Daphnia pulex*), Hitam (*Heterotrigona itama*), Lmigr (*Locusta migratoria*), Cmoro (*Carausius morosus*), Sgreg (*Schistocerca gregaria*), Lsalm (*Lepeophtheirus salmonis*), Alabo (*Apis laboriosa*). Species within the blue area possess highly conserved mature peptide sequences, whereas those in the magenta zone exhibit relatively less conservation in their mature peptides.

(B) Schematic organization of CRZ precursors in representative species. Signal peptides (blue)

260 and mature CRZ peptides (red) are indicated.

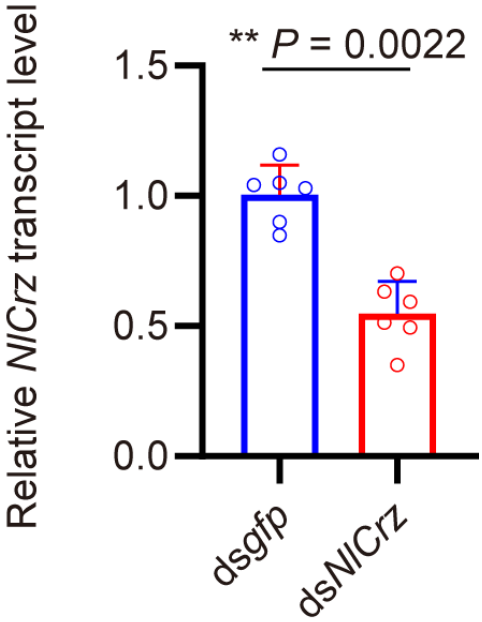

261

262 **Figure 1 - figure supplement 2.** The *Crz* gene-silencing efficacy in female insects following
263 dsRNA injection assayed by qPCR. The small circles denote the number of replicates. Data
264 are shown as mean ± s.e.m. Mann–Whitney test. ***P*<0.001.

265

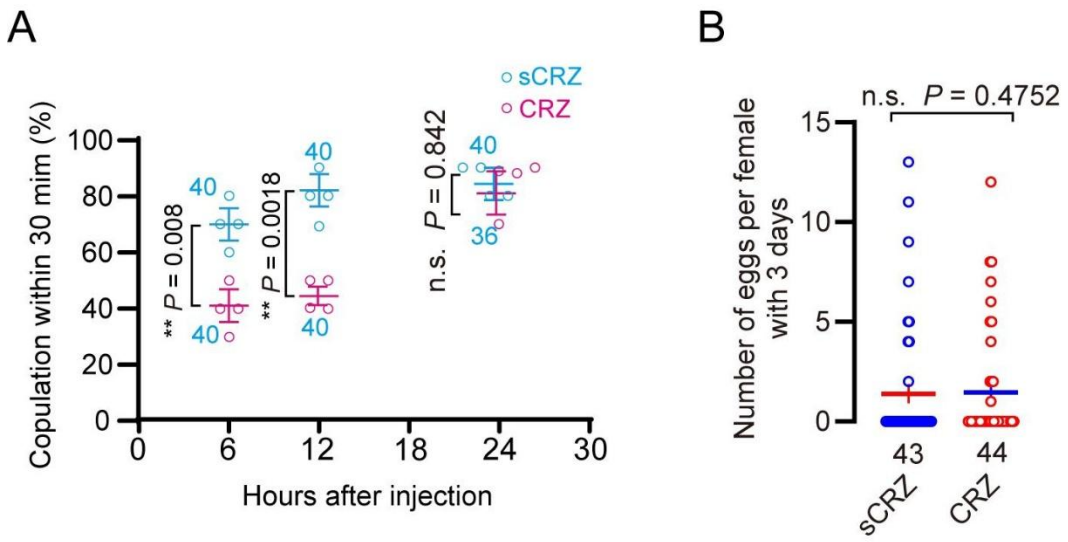

Figure 1 - figure supplement 3. Phenotypic effects of CRZ peptide injection.

(A) Receptivity of virgin females at indicated time points after CRZ injection (sCRZ as control). Each virgin female BPH was injected with a calibrated glass capillary needle directly into the abdomen with 100 ng of peptide dissolved in 50 nL of 1 × PBS balanced salt solution. Graph shows percentage females copulating within 30 min. ** $P < 0.01$; ns: not significant Binomial, GLM with logit link, followed by pairwise contrasts. The small circles denote the number of replicates, ≥8 insects/replicate; the numbers associated with the curves denote total number of animals.

(B) Eggs laid per virgin female after neuropeptide injection (sCRZ, control). Females were mated with wild-type males for 12 h prior to assessment. Each virgin female BPH was injected with a calibrated glass capillary needle directly into the abdomen with 100 ng of peptide dissolved in 50 nL of 1 × PBS balanced salt solution. Data are shown as mean ± s.e.m. ns: $P > 0.05$ (Student's t-test). The numbers below the bars denote total number of animals, ≥4 biological replicates, ≥10 insects/replicate).

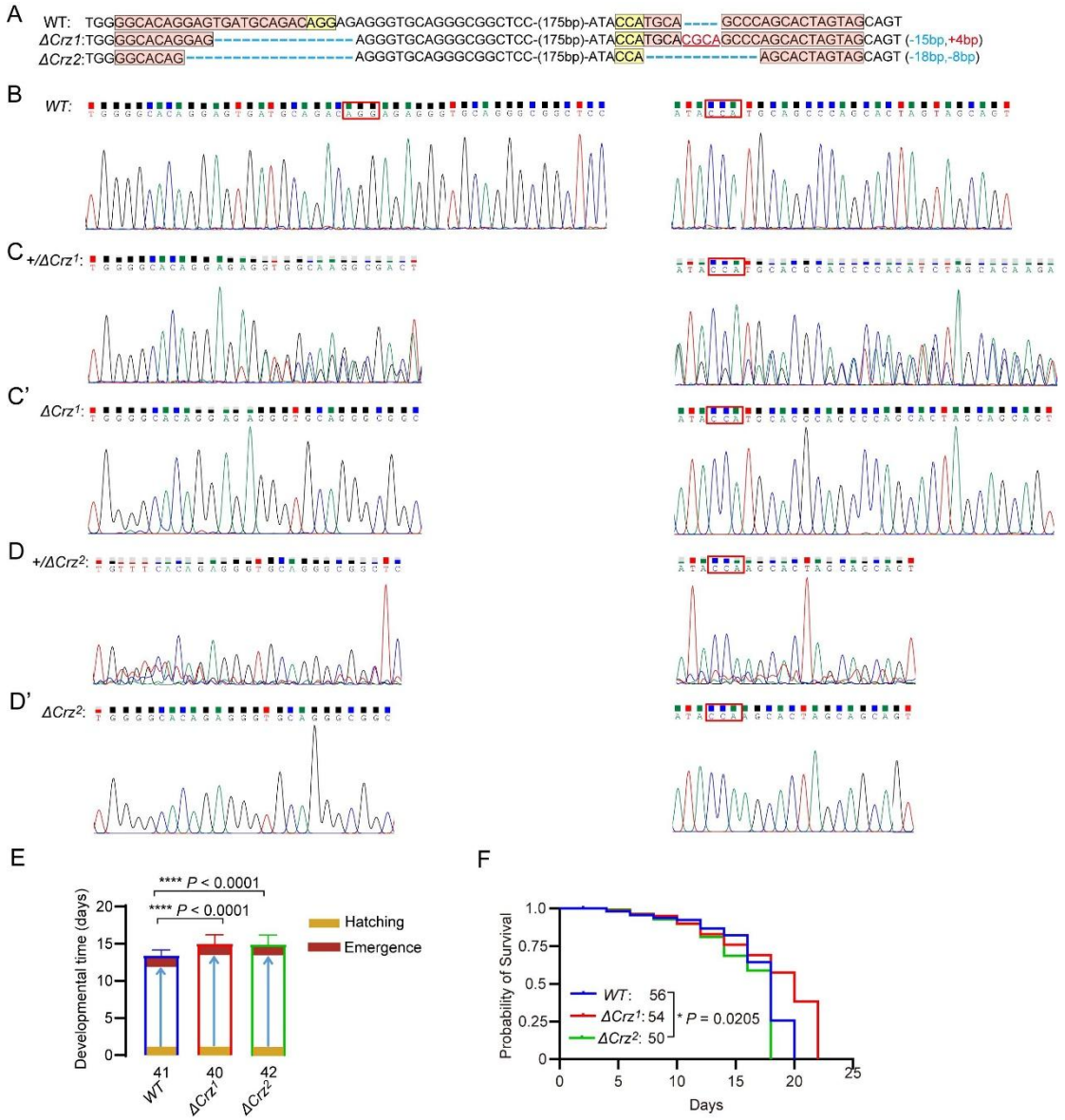

Figure 1 - figure supplement 4. Characterization of *Crz* mutants in *N. lugens*.

(A) Sequencing of *Crz* mutant (*ΔCrz¹* and *ΔCrz²*) and wild type (WT) PCR products from BPHs. The exact indel types of the G0 mutant individuals were confirmed by cloning and sequencing. The wild-type sequences are shown at the top with the target site marked by in pink shading and PAM in yellow shading. The change in the length of the mutant sequence is shown on the right side of the sequence (+, insertion; -, deletion). (B) The Sanger sequence chromatograms flanking the sgRNA target site for wild type (WT). (C and D) The Sanger sequence chromatograms flanking the sgRNA target site for wild type (WT), heterozygous mutant ($\Delta Crz^{1/+}$ and $\Delta Crz^{2/+}$). (C' and D') The Sanger sequence chromatograms flanking the sgRNA target site for wild type (WT), homozygous mutant (*ΔCrz¹* and *ΔCrz²*).

(E) Developmental duration (egg to adult) across genotypes. ****P < 0.0001 (Student's *t*-test). The numbers below the bars denote total number of animals. (F) Survival curves of adult *Crz* mutants vs. WT. *P < 0.05 (Log-rank Mantel-Cox test; df = 1; n ≥ 50/group).

295 **CRZ is produced by similar neurons in both sexes of BPHs and is**
296 **absent from the male accessory gland**

297 To further understand how CRZ regulates the PMR in BPHs, we examined the
298 expression of CRZ and *Crz* across different tissues in males and females. The *Crz*
299 mRNA expression was examined in various BPH tissues using both RT-PCR and
300 qPCR (Figure 2A). We detected *Crz* mRNA expression primarily in the central
301 nervous system (CNS), regardless of the primer set or detection method used, while
302 expression was nearly undetectable in other tissues, including reproductive organs of
303 both sexes (Figure 2B and C).

304 A previous study reported CRZ in four male-specific interneurons within the
305 abdominal ganglia of *D. melanogaster* [47]. To determine whether CRZ exhibits sexually
306 dimorphic expression in BPHs, we performed immunolabeling using an anti-CRZ
307 antiserum. This labeled four pairs of neurons in the protocerebrum of the brain (Figure
308 2D and E) and one pair of neurons in the subesophageal ganglion in both males and
309 females (Figure 2D and E). Since CRZ immunolabeled neurons in brains of most, if
310 not all, insects studied include three or more pairs of lateral neurosecretory cells [55,56],
311 we suggest that CRZ signaling regulating the PMR may be hormonal (at least in part).
312 Importantly, no CRZ-immunopositive neurons were detected in the abdominal ganglia
313 of either sex (Figure 2D and E), and thus there is no evidence for sex-specific
314 expression of CRZ in neurons in BPHs. This is in contrast to *D. melanogaster*, where
315 we confirmed, as previously reported [45], the presence of CRZ-immunolabeled
316 neurons specifically in the abdominal ganglia of males (Figure 2 - figure supplement

317 1A).

318 To exclude that CRZ acts as a seminal fluid peptide transferred to females during
319 copulation, similar to sex peptide (SP) in *D. melanogaster* and macc in BPHs [24], we
320 specifically examined CRZ expression in reproductive tissues of both sexes. However,
321 we observed no CRZ immunolabeling in the male reproductive organs (Figure 2F1 -
322 F3) or female reproductive organs (Figure 2G1 – G3). This aligns with our
323 transcriptional *Crz* data shown above (Figure 2B and C). Furthermore, *Crz* mRNA and
324 CRZ protein were absent from transcriptomic and proteomic datasets of the male
325 accessory glands (MAGs) in BPHs [24]. Collectively the available data suggest, that
326 CRZ is not produced by the MAG and is consequently unlikely to be transferred to
327 females as a seminal fluid component.

328

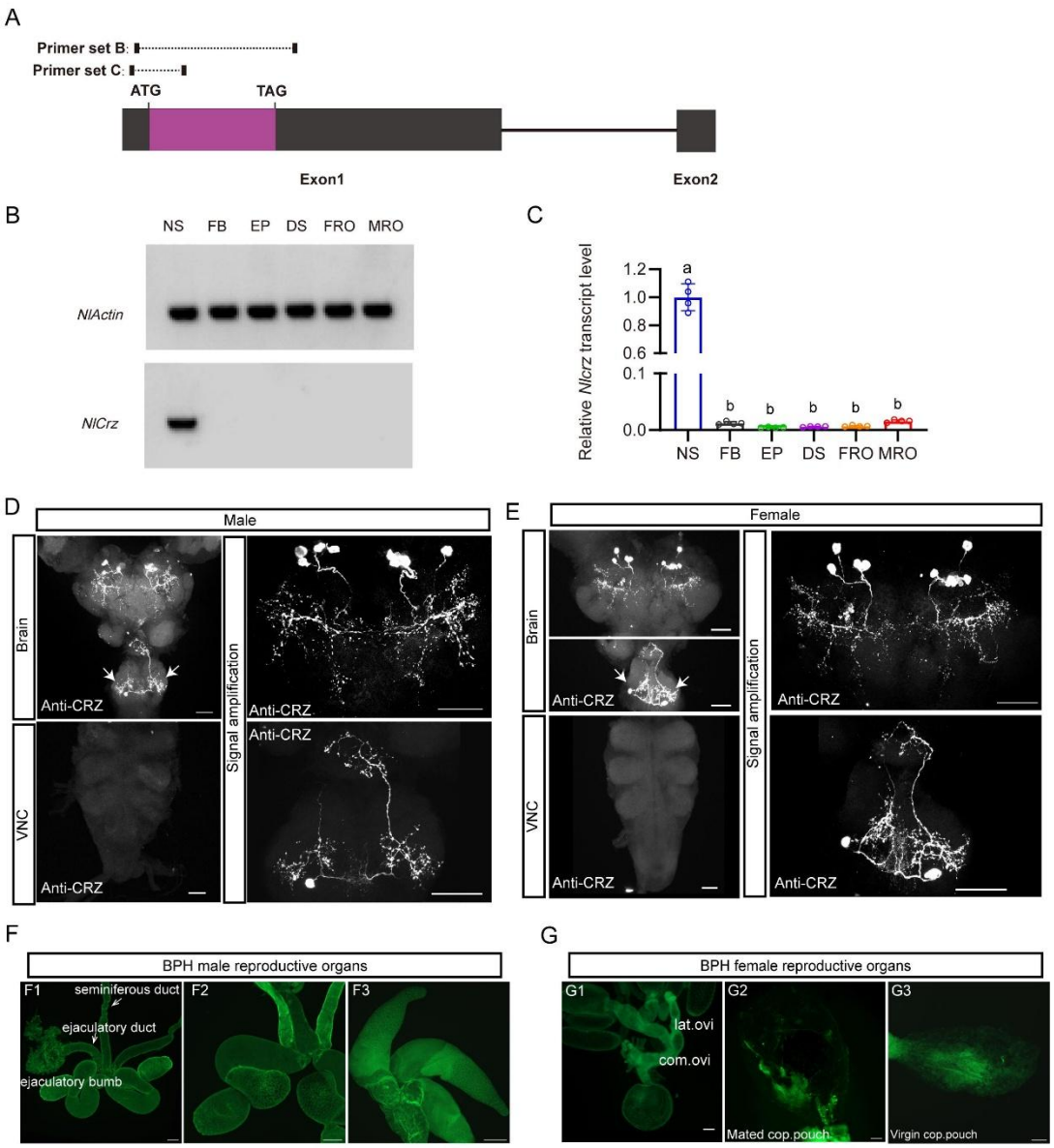

Figure 2. Expression of *Crz* and CRZ in the nervous system of the brown planthopper (BPH). (A) Schematic of primer design for *Crz* detection (primer sequences provided in Table S1). (B) RT-PCR analysis of *Crz* mRNA levels in various BPH tissues. Actin served as the loading control. Tissues: Nervous system (NS), fat body (FB), Epidermis (EP), digestive system (DS), female reproductive organs (FRO), male reproductive organs (MRO). Note: Tissues except reproductive organs were pooled from both sexes.

(C) Relative *Crz* expression in female *N. lugens* tissues determined by RT-qPCR (abbreviations as in B). Expression was normalized to *Actin* and *18SrRNA* and expressed relative to the mean value of the highest-expressing tissue (set to 1). Data are shown as mean ± s.e.m. Groups that share at least one letter are statistically indistinguishable. One-way ANOVA followed by Tukey's multiple comparisons test.

(D and E) Immunolocalization of CRZ peptide in the nervous system of male (D) and female (E) BPHs. Four pairs of CRZ neurons in the brain and one pair in the subesophageal ganglion are

343 shown. Note that some of the CRZ neurons are likely to be neurosecretory cells with axon
344 terminations in the corpora cardiaca, others may be interneurons. The extensive branches
345 within the brain suggest CRZ signaling in brain circuits. VNC, ventral nerve cord. Scale bars:
346 50 μm. (E) CRZ immunolabeling in the nervous system of female BPHs. Scale bar: 50 μm.
347 (F and G) Lack of CRZ immunoreactivity in BPH reproductive organs. (F1-F3) Male
348 reproductive organs (MRO): testes (test). (G1-G3) Female reproductive organs (FRO): lateral
349 oviduct (Lat. ov), common oviduct (Com. ov). Scale bars: 100 μm.
350

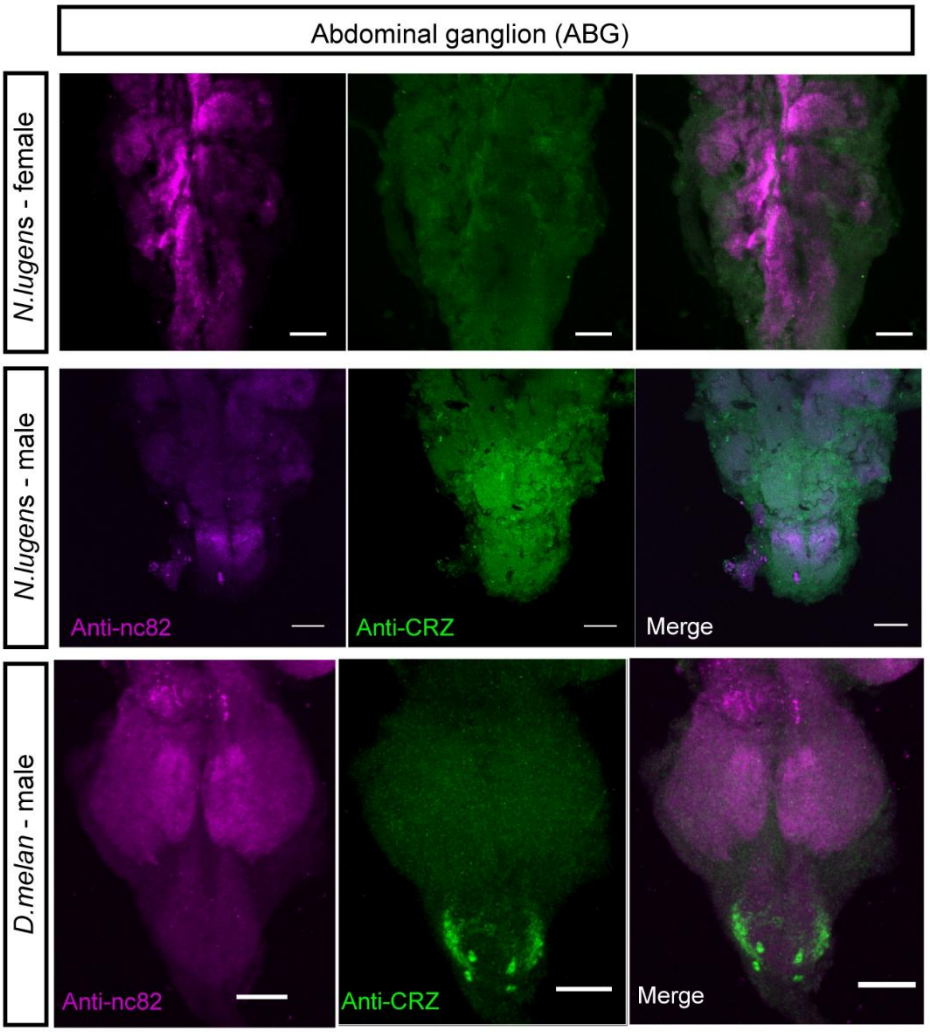

351

352 **Figure 2 - figure supplement 1.** CRZ immunolabeling in abdominal ganglion and
353 reproductive organs of male and female BPHs and *D. melangaster*.
354 Anti-CRZ immunolabeling in the abdominal ganglia of the ventral nerve cord (VNC) in *N.*
355 *lugens* and *D. melanogaster* (*D. Melan.*). Scale bar: 50 μm. Note: Male-specific CRZ-positive
356 neurons are present in *D. melanogaster*, as previously reported.

357 **The CRZ receptor is essential for mediating the post mating**

358 **response in female BPHs**

359 Given our findings implicating CRZ in modulating the PMR in female BPHs, we
360 identified the CRZ receptor (*CrzR*) gene in this species; it encodes a structurally
361 conserved GPCR orthologous to other insect *CrzR*s (Figure 3-supplemental figure 1).
362 We next explored the effect of knocking down the *CrzR* on the PMR in BPHs.
363 RNAi-mediated knockdown of the receptor (*dsCrzR* injection) resulted in 15% of the
364 mated females re-mating, a phenotype not seen in *dsgfp*-injected controls (Figure 3A
365 and B) and in significantly reduced oviposition (Figure 3C). Importantly, CRZ injection
366 failed to diminish receptivity in *CrzR*-knockdown virgins (Figure 3D and E).
367 Furthermore, MAG extract (with seminal fluid proteins) injection into *dsCrzR*-treated
368 virgins did not affect receptivity (Figure 3F).

369 To further confirm the role of the *CrzR* in the PMR of BPHs, we applied
370 CRISPR/Cas9 genome editing to mutate the *CrzR* gene and constructed a
371 homozygous mutant strain of *CrzR* ($CrzR^{M}$) by genetic crosses (Figure 3G-3G'', Fig. 3
372 - figure supplement 2A). We found that the developmental time and life span of the
373 female *CrzR* mutants, like the *Crz* mutants, were slightly extended compared to wild
374 type animals (Figure 3 - supplement figure 2E and 2F). Homozygous $CrzR^{M}$ females
375 displayed increased remating rates (30%) (Figure 3I and J) and the number of eggs
376 laid by $CrzR^{M}$ females was also significantly decreased (Figure 3K). We also
377 examined mating and oviposition behaviors in *CrzR* heterozygous (+/$CrzR^{M}$) females.
378 Notably, both the remating rate and egg production in heterozygous females were

379 comparable to those observed in homozygous *CrzR* mutant (*CrzR*^{M}) females
380 (approximately 30%) (Figure 3I and J). Thus, heterozygosity for the *CrzR* was
381 sufficient to disrupt post-mating behaviors in female BPHs. These findings indicate
382 that the *CrzR* loss-of-function phenotype is dominant, and that a single functional
383 copy of *CrzR* is insufficient to maintain a normal post-mating response. Consistent
384 with the *CrzR* RNAi results, neither CRZ nor MAG extract injections reduced
385 receptivity in *CrzR*^{M} virgins (Figure 3K - M). Finally, macc peptide injection also failed
386 to decrease receptivity in *CrzR*-mutant virgins (70% acceptance rate), whereas it
387 significantly suppressed mating in wild-type controls (Figure 3N). These results
388 collectively demonstrate that intact CRZ/*CrzR* signaling in female BPHs is required for
389 transducing the PMR-inducing effects of male-derived seminal factors, including macc
390 [24].
391

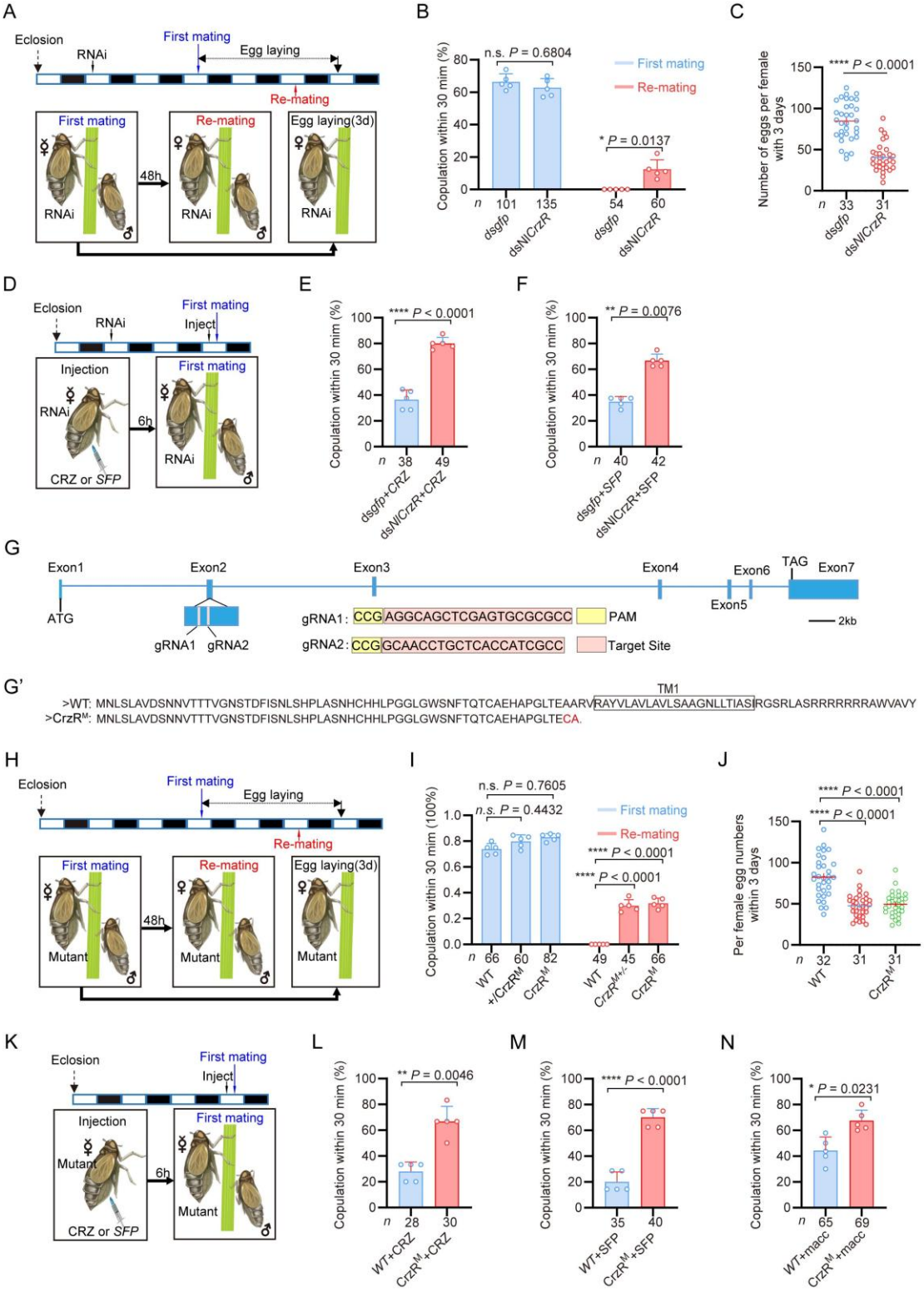

Figure 3. The CRZ receptor (*CrzR*) is essential for the female PMR and is required for action of MAG-derived factors**.**

(A) Experimental design for B and C.

(B) Receptivity after *CrzR*-RNAi (injection of ds*CrzR*; ds*GFP* as control). Percentage females

398 copulating within 30 min. The small circles denote the number of replicates, ≥9
399 insects/replicate; the numbers below the bars denote total number of animals. Statistical
400 comparisons of proportions were performed using chi-square tests for contingency tables, $P <$
401 0.05 was considered significant.
402 (C) Numbers of eggs laid within 72 h post-mating (*dsCrzR* females × WT males). Data are
403 shown as mean ± s.e.m. ****$P < 0.0001$ (Student's *t*-test). The numbers below the bars denote
404 total number of animals, ≥4 biological replicates, ≥7 insects/replicate.
405 (D) Experimental design for E-F.
406 (E) Receptivity after CRZ injection in *CrzR*-knockdown virgins (*dsGFP* + CRZ control). Graph
407 shows percentage females copulating within 30 min. Each virgin female BPH was injected with
408 a calibrated glass capillary needle directly into the abdomen with 10 ng of peptide dissolved in
409 50 nL of 1 × PBS balanced salt solution. The small circles denote the number of replicates, ≥7
410 insects/replicate; the numbers below the bars denote total number of animals. Statistical
411 comparisons of proportions were performed using chi-square tests for contingency tables, $P <$
412 0.05 was considered significant.
413 (F) Receptivity after MAG extract (with seminal fluid proteins) injection in *CrzR*-knockdown
414 virgins (*dsGFP* + SFP control). Percentage copulating within 30 min. The small circles denote
415 the number of replicates, ≥7 insects/replicate; the numbers below the bars denote total
416 number of animals. Statistical comparisons of proportions were performed using chi-square
417 tests for contingency tables, $P < 0.05$ was considered significant.
418 (G) *CrzR* targeting strategy for generation of mutants. *Top:* Genomic structure (ATG/TAG in
419 Exons 2/7). sgRNA target (pink), PAM (yellow). *Bottom:* CRISPR alleles.
420 (G') Translated receptor mutant sequences.
421 (H) Experimental design for I-J.
422 (I) Receptivity of *CrzR* mutants compared to wild type animals (WT). Graph displays the
423 percentage of females copulating within 30 min. The small circles denote the number of
424 replicates, ≥9 insects/replicate; the numbers below the bars denote total number of animals.
425 Statistical comparisons of proportions were performed using chi-square tests for contingency
426 tables, $P < 0.05$ was considered significant.
427 (J) Number of eggs laid by mutants mated with WT males within 72 h. The numbers below the
428 bars denote total number of animals, ≥4 biological replicates, ≥7 insects/replicate. Data are
429 shown as mean ± s.e.m. ****$P < 0.0001$; Student's *t* test.
430 (K) Experimental design for L-M.
431 (L) Receptivity after CRZ injection in *CrzR* mutants compared to WT. Graph displays the
432 percentage of females copulating within 30 min. Each virgin female BPH was injected with a
433 calibrated glass capillary needle directly into the abdomen with 10 ng of peptide dissolved in
434 50 nL of 1 × PBS balanced salt solution. The small circles denote the number of replicates, ≥5
435 insects/replicate; the numbers below the bars denote total number of animals. Statistical
436 comparisons of proportions were performed using chi-square tests for contingency tables, $P <$

0.05 was considered significant.

(M) Receptivity after SFP injection in *CrzR* mutants compared to WT. Graph displays the percentage of females copulating within 30 min. The small circles denote the number of replicates, ≥7 insects/replicate; the numbers below the bars denote total number of animals. Statistical comparisons of proportions were performed using chi-square tests for contingency tables, $P < 0.05$ was considered significant.

(N) Receptivity after macc injection in *CrzR* mutants compared to WT. Graph displays the percentage of females copulating within 30 min. The small circles denote the number of replicates, ≥10 insects/replicate; the numbers below the bars denote total number of animals. Statistical comparisons of proportions were performed using chi-square tests for contingency tables, $P < 0.05$ was considered significant.

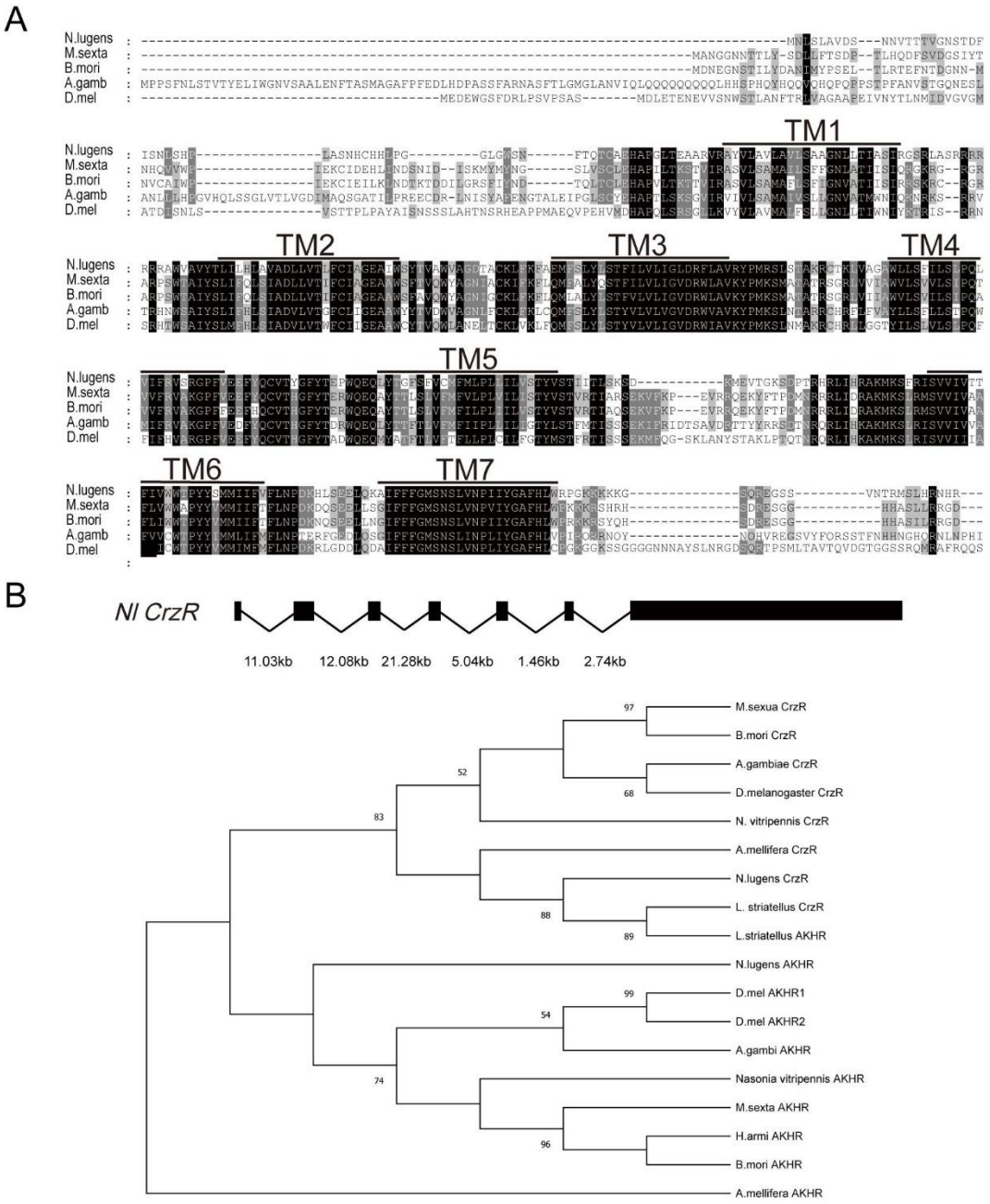

449 **Figure 3 - figure supplement 1**. Structural conservation of the *CrzR* across insect species.
450 (A) Multiple sequence alignment highlighting conserved transmembrane domains (TM1-TM7,
451 shaded) in CRZ receptor orthologs. The species shown are: *N. lugens*: *Nilaparvata lugens; M.*
452 *sexta: Manduca sexta; B. mori*: *Bombyx mori*; *A. gamb*: *Anopheles gambiae*; *D. mel*: *D.*
453 *melanogaster*.
454 (B) Phylogenetic analysis of *CrzR* and *AkhR* based on the alignment of amino acid sequences
455 of insect species. Phylogenetic analysis was performed in MEGA 12 using the Maximum
456 Likelihood method with the LG amino-acid substitution model and Gamma-distributed rate
457 variation among sites (G, 5 discrete categories), with gaps treated by complete deletion.
458 Branch support was evaluated with 10,000 bootstrap replicates, and the numbers at the nodes
459 indicate bootstrap support values.

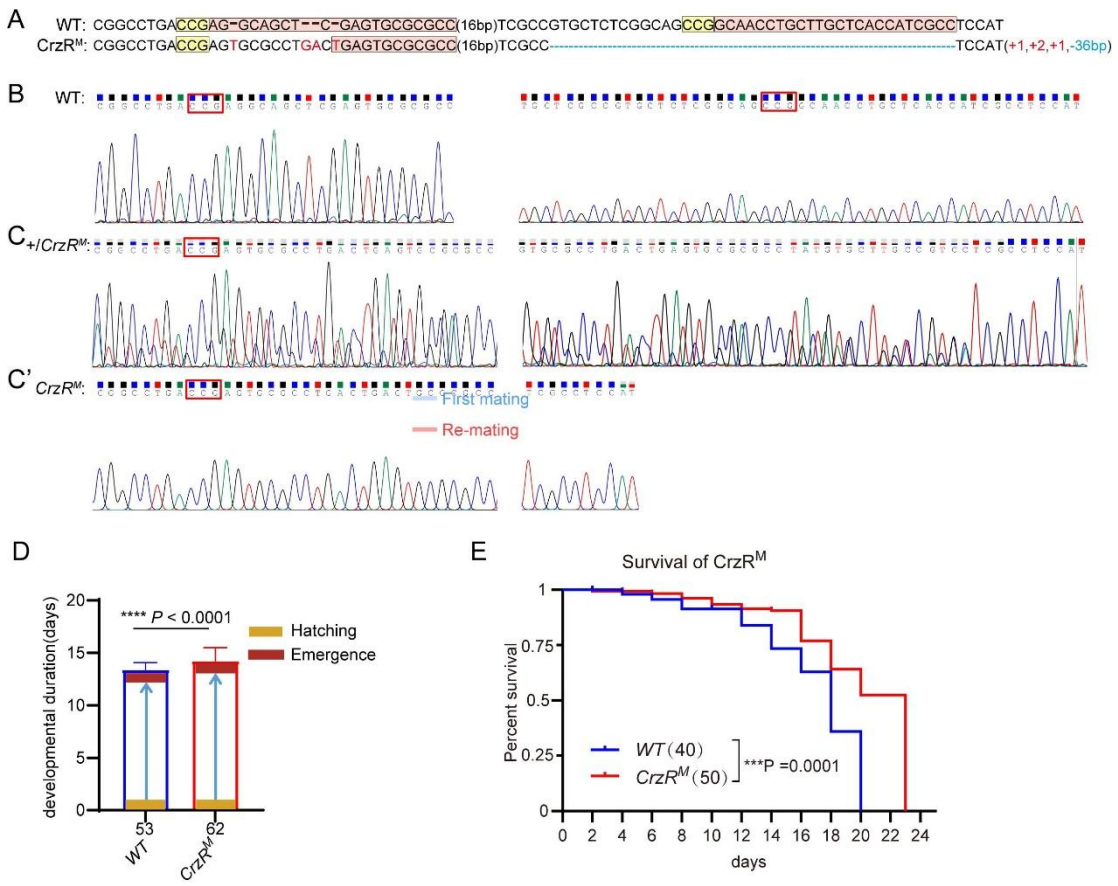

Figure 3 - figure supplement 2. Characterization of *CrzR* mutants in *N. lugens*.

(A) Sanger sequencing of *CrzR* mutants. WT sequence with target (pink), PAM (yellow). Indels: + (insertion), – (deletion).

(B) Sanger sequencing chromatograms of *CrzR* alleles: WT (wild-type).

(C) Sanger sequencing chromatograms of *CrzR* alleles: heterozygous ($CrzR^{M/+}$).

(C') Sanger sequencing chromatograms of *CrzR* alleles: homozygous ($CrzR^{M}$) mutants.

(D) Developmental duration (egg to adult eclosion) in *CrzR* mutants compared to WT. Data: mean ± SD. ****$P < 0.0001$ (Student's *t*-test; n ≥ 40/group).

(E) Survival curves of adult *CrzR* mutants compared to WT. ***$P < 0.001$ (Log-rank Mantel-Cox test; df = 1; n ≥ 50/group).

472 **The *CrzR* is highly expressed in the reproductive organs of female BPHs**

473 To further elucidate the role of the CRZ signaling in regulation of the PMR, we
474 analyzed the *CrzR* expression in *N. lugens* tissues. We first monitored *CrzR*
475 expression by means of RT-PCR and qPCR. Both methods revealed predominant
476 *CrzR* transcript expression in the female reproductive tract (Figure 4A-C). qPCR
477 further demonstrated significantly higher *CrzR* expression in adult females than in
478 males (Figure 4 - figure supplement 1A), particularly localized to female abdomens
479 (Figure 4 - figure supplement 1B).

480 As we failed to generate a functional NlCrzR antibody, to determine the tissue
481 expression of the receptor in more detail, we used *in situ* hybridization and confirmed
482 strong *CrzR* expression within the female reproductive system (Figure 4D). No
483 hybridization signal was detected in the lateral or common oviducts (Figure 4D1).
484 However, specific labeling occurred in the sperm storage organs: the spermathecae
485 and pouched glands of the lower reproductive tract (Figure 4D2 and 4D2'). These
486 structures are the primary sites for long-term sperm storage. Specificity was validated
487 by absence of signal in sense-probe controls (Figure 4D3 - D4'). This enrichment in
488 sperm storage organs suggests that CRZ signaling may modulate post-mating
489 physiology in part by regulating the mobilization of stored sperm and seminal fluid.

490 Notably, while CrzR is highly expressed in the female reproductive tract, we
491 acknowledge that RT-PCR and qPCR analyses also detected low but detectable CrzR
492 expression in other tissues, including the CNS and fat body (Figure 4B-C). Thus, we
493 cannot exclude the possibility that *CrzR* in the brain (e.g., by modulating neural

494 circuits governing reproductive behavior) or fat body (e.g., by affecting post-mating
495 metabolism and nutrient/energy allocation) may also contribute to the PMR. These
496 non-reproductive tract sites of CrzR expression warrant further investigation to fully
497 delineate the systemic roles of CRZ/CrzR signaling in female PMR regulation.
498

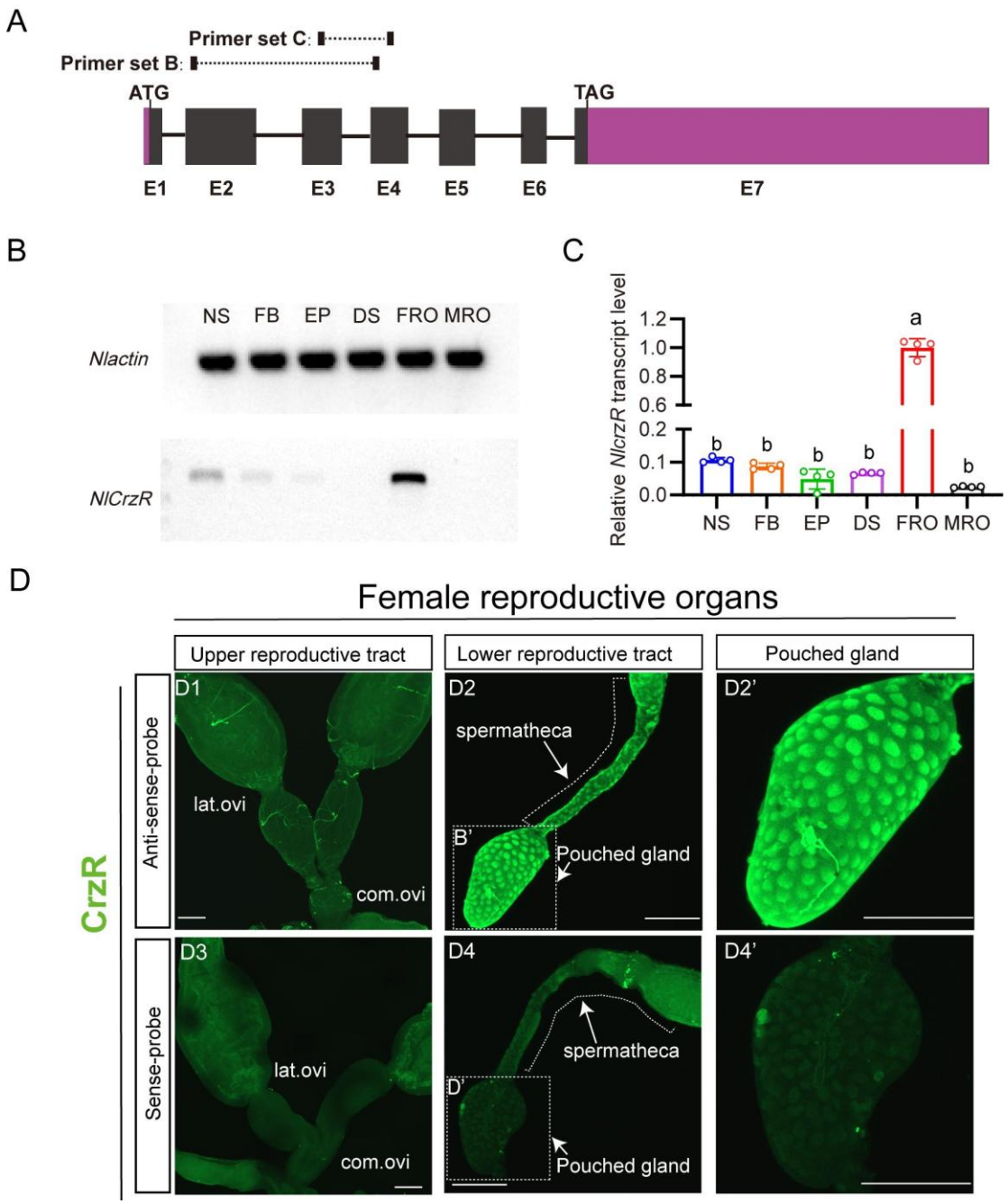

Figure 4. Spatial expression profiling of *CrzR* in the female *N. lugens* reproductive tract.

(A) *CrzR* genomic structure with primer design for experiments in panels B-C.

(B) RT-PCR analysis of *CrzR* tissue distribution. Note weaker expression in central nervous system and fat body. Actin loading control is shown in top row. Tissue abbreviations: NS: central nervous system; FB: fat body; EP: Epidermis; DS: digestive system, FRO: female reproductive organs, MRO: male reproductive organs. Except for the reproductive system, the rest of the tissues come from a mixture of female and male.

(C) Relative *CrzR* expression in female *N. lugens* tissues determined by RT-qPCR (abbreviations as in B). Expression was normalized to *Actin* and *18SrRNA* and expressed relative to the mean value of the highest-expressing tissue (set to 1). Data are shown as mean ± s.e.m. Groups that share at least one letter are statistically indistinguishable. One-way

ANOVA followed by Tukey's multiple comparisons test.

(D1 - D2') *CrzR* mRNA localization via fluorescent *in situ* hybridization (antisense probe): D1: There is no signal in lateral/common oviducts; D2/D2': Specific signal is detected in spermatheca (SP) and pouched gland (PG).

(D3 - D4') Negative controls (sense probe) showing background-level signal. Scale bars: 100 µm.

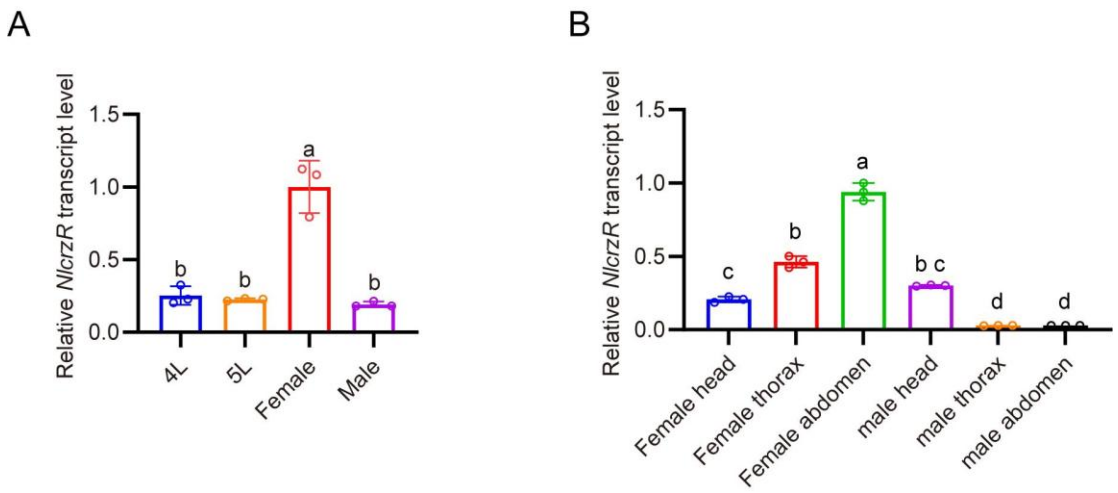

Figure 4 - figure supplement 1. Developmental and tissue-specific expression profiling of *CrzR* in *N. lugens* determined by qPCR.

(A) *CrzR* transcript levels across developmental stages. Relative expression levels were quantified by RT-qPCR, normalized to the reference gene *Actin*, expressed relative to the mean value of the highest-expressing tissue (set to 1). Data are shown as mean ± SEM shown. Groups that share at least one letter are statistically indistinguishable. One-way ANOVA followed by Tukey's multiple comparisons test.

(B) *CrzR* expression in distinct body regions. Relative expression levels were quantified by RT-qPCR, normalized to the reference gene *Actin*, expressed relative to the mean value of the highest-expressing tissue (set to 1). Data are shown as mean ± SEM shown. Groups that share at least one letter are statistically indistinguishable. One-way ANOVA followed by Tukey's multiple comparisons test.

532 **Endogenous CRZ signaling modulates aspects of the PMR in female**
533 ***Drosophila melanogaster***

534 Having established the critical role of CRZ signaling in regulating the PMR of the
535 female BPH, we next investigated its potential function in female reproduction,
536 including the PMR, of the genetically tractable fly *D. melanogaster*.

537 We first assessed re-mating frequency in *Crz* mutant female flies (Crz^{attp}).
538 Approximately 40% of the Crz^{attp} females that had experienced a first successful
539 copulation mated again, compared to only 3% of mated wild-type control females
540 (Figure 5A and B). Importantly, the *Crz* mutation did not affect the first mating of
541 females (Figure 5B). Furthermore, mated Crz^{attp} females laid approximately 45%
542 fewer eggs than mated wild-type females (Figure 5C). These results demonstrate that
543 CRZ signaling is necessary for aspects of the PMR in female *D. melanogaster*,
544 specifically inhibiting re-mating and stimulating post-mating egg production.
545 Immunohistochemical labeling confirmed the absence of CRZ protein in Crz^{attp}
546 mutants (Figure 5D).

547 To determine whether release of CRZ from *Crz* neurons is responsible for
548 inhibition of remating and stimulation of oviposition, we knocked down *Crz* expression
549 specifically in CRZ-producing neurons using the GAL4-UAS system (*Crz-GAL4* >
550 *UAS-Crz-RNAi*). Consistent with the mutant phenotype, 22% of the mated *Crz-GAL4* >
551 *UAS-Crz-RNAi* females mated again after their first successful mating with wild-type
552 males, whereas only 2% of the control females (*Crz-GAL4/+*) did so (Figure 5E).
553 Virgin receptivity was again unaffected by *Crz* knockdown (Figure 5E). Additionally,

554 mated *Crz-GAL4* > *UAS-Crz-RNAi* females laid approximately 20% fewer eggs than
555 mated controls (*Crz-GAL4/+*) (Figure 5F). To further confirm the role of CRZ
556 neuropeptide in modulation of the PMR in females, we injected this peptide in virgin
557 females. Consistent with the above results, CRZ injected virgins displayed a reduced
558 response to mating attempts (Figure 5G). To determine whether CRZ modulates the
559 PMR endogenously also in female *D. melanogaster*, we first examined whether the
560 male accessory gland (MAG) expresses *Crz*. RT-PCR analysis revealed no
561 detectable *Crz* transcripts in the *D. melanogaster* MAG (Figure 5H), indicating that the
562 MAG does not synthesize the CRZ peptide. To further exclude the possibility that CRZ
563 or any other *Crz*-precursor-derived peptide might enter the AG from other sources, we
564 used the GAL4–UAS system to visualize *Crz*/CRZ-producing neurons and performed
565 immunolabeling with anti-CRZ antibodies. Neither approach revealed any signal in the
566 MAG (Figure 5I). Some GFP signals were observed in cells of the testes (indicated by
567 white arrows), whereas no corresponding signal was detected by CRZ
568 immunohistochemistry (Figure 5I).

569 To further evaluate whether the MAG could be a source of CRZ, we interrogated
570 publicly available single-cell transcriptomic datasets from the Fly Cell Atlas covering
571 the male reproductive glands (including MAG main and secondary cells, ejaculatory
572 duct/bulb epithelium, secretory and muscle cells) and the male testis (Figure 5 - figure
573 supplement 1). In the MAG atlas, *Crz* transcripts were undetectable across MAG main
574 and secondary cells as well as other gland-associated cell types (Figure 5 - figure
575 supplement 1A). In contrast, the MAG-derived sex peptide (SP) was robustly detected,

576 confirming correct tissue representation and cell-type annotation (Figure 5 - figure
577 supplement 1A). In the testis atlas, Crz expression was sparse and restricted to a
578 small subset of cells rather than enriched in any major spermatogenic lineage (Figure
579 5 - figure supplement 1B and C), whereas β2-tubulin prominently marked
580 spermatogenic populations (Figure 5 - figure supplement 1B). Hence, these
581 single-cell data support our RT-PCR and anti-CRZ immunolabeling findings. Together,
582 our data demonstrate that the male accessory gland does not produce or sequester
583 CRZ. In conclusion, like in BPHs, CRZ acts endogenously in females to modulate
584 post-mating behavior also in *D. melanogaster*.
585
586

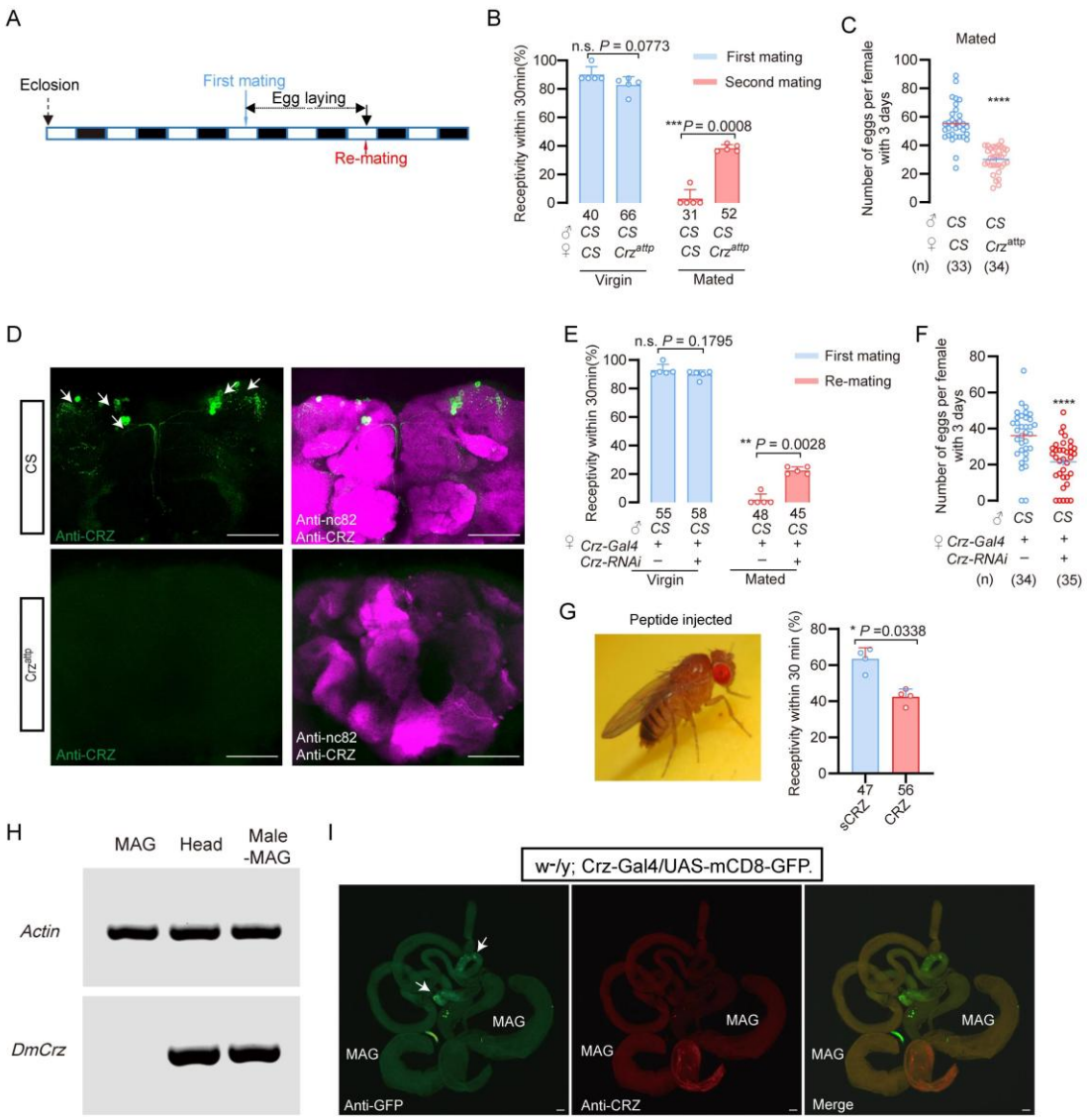

587

588 **Figure 5**. CRZ regulates part of the PMR in *D. melanogaster*.

589 (A) Schematic of experimental design. White segments on the time axis indicate light periods;
590 black segments indicate dark periods.

591 (B) Receptivity of virgin and mated *Crz* mutant (*Crz*^{attp}) females. Graph displays the
592 percentage of females copulating within 30 min. Small circles indicate the number of replicates,
593 ≥6 insects/replicate; numbers below bars denote total number of animals. Statistical
594 comparisons of proportions were performed using chi-square tests for contingency tables, $P <$
595 0.05 was considered significant.

596 (C) Graph shows eggs laid per female after mating. Numbers below bars denote total animals,
597 ≥4 biological replicates, ≥8 insects/replicate. ****$P < 0.0001$ (Student's t-test).

598 (D) Anti-CRZ immunostaining in brains of *Crz* mutant (*Crz*^{attp}), control (Cs) and after *Crz*-RNAi).
599 Note CRZ-expressing cells at arrows in control. Scale bar: 100 μm.

600 (E) Receptivity of virgin and mated females after *Crz*-RNAi. Graph displays the percentage of
601 females copulating within 30 min. Small circles indicate the number of replicates, ≥8

602 insects/replicate; numbers below bars denote total animals. Statistical comparisons of
603 proportions were performed using chi-square tests for contingency tables, $P < 0.05$ was
604 considered significant.
605 (F) Graph shows eggs laid per female after mating. Numbers below bars denote total animals,
606 ≥4 biological replicates, ≥8 insects/replicate. ****$P < 0.0001$ (Student's *t*-test).
607 (G) Receptivity of virgin females following CRZ peptide injection (monitored 6 h after injection).
608 Graph displays the percentage of females copulating within 30 min. Small circles indicate the
609 number of replicates, ≥9 insects/replicate; numbers below bars denote total animals. Statistical
610 comparisons of proportions were performed using chi-square tests for contingency tables,$P <$
611 0.05 was considered significant.
612 (H) RT-PCR analysis of Crz tissue distribution. Note the lack of expression in the accessory
613 gland. Actin loading control is shown in the top row. Tissue abbreviations: MAG, male
614 accessory gland; Male–MAG, whole body without male accessory gland.
615 (I) Anti-GFP and anti-CRZ immunostaining in brains of *w⁻/y; Crz-Gal4/UAS-mCD8-GFP*. Note
616 no signal was detected in male accessory gland (MAG). Some GFP-stained signals were
617 observed in the testes (indicated by white arrows), whereas no corresponding signals were
618 detected via CRZ antibody staining. Scale bar: 50 μm.

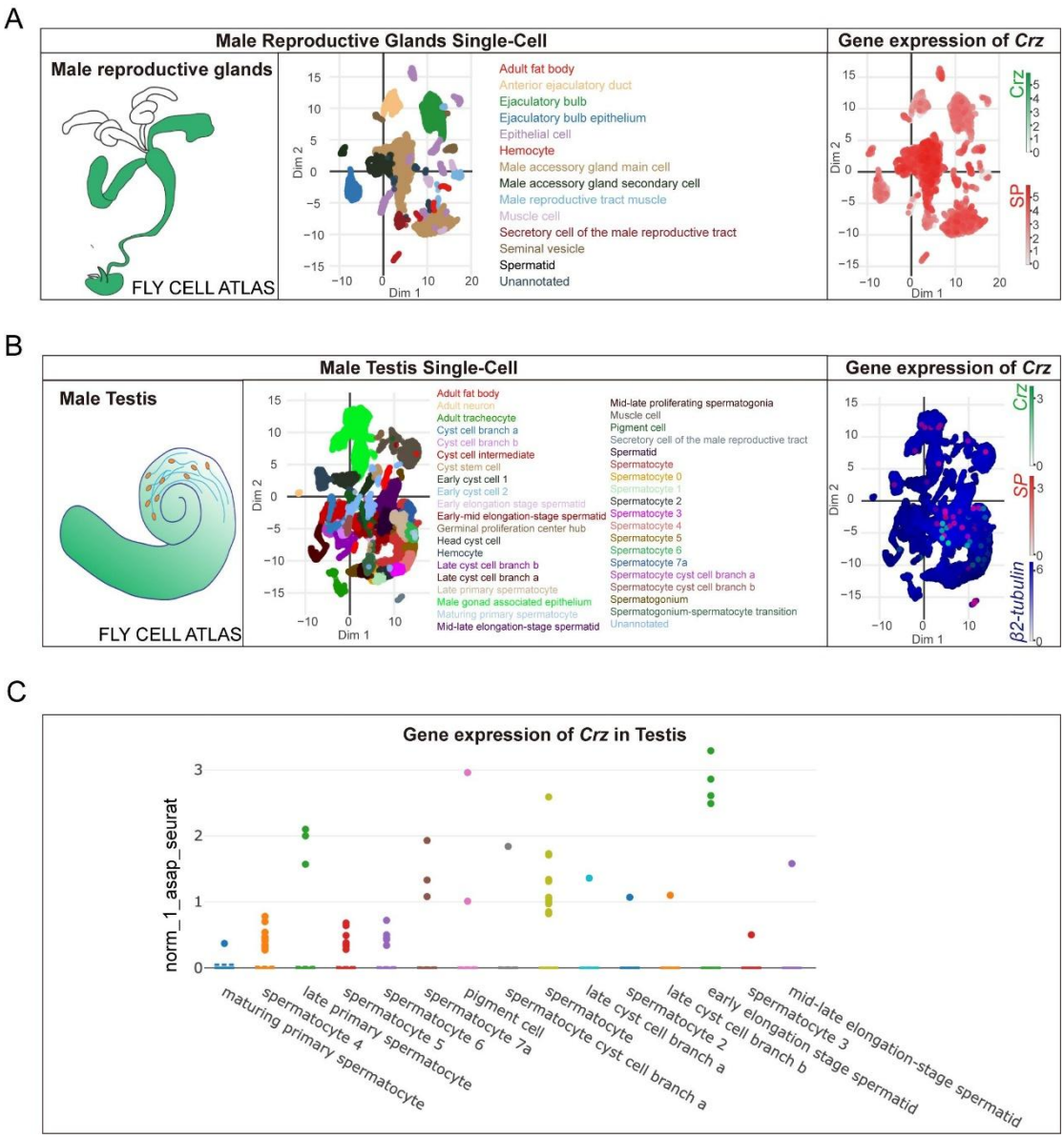

Figure 5 - figure supplement 1. Crz expression is undetectable in the *Drosophila* male accessory gland in Fly Cell Atlas single-cell datasets.

(A) Fly Cell Atlas male reproductive glands single-cell dataset. Left, schematic of male reproductive glands. Middle, two-dimensional embedding colored by annotated cell types, including male accessory gland (MAG) main and secondary cells. Right, feature plot showing expression of Crz (green scale) together with the AG marker sex peptide (SP) (red scale). Crz transcripts are not detected in MAG cell populations, whereas SP is robustly expressed.

(B) Fly Cell Atlas male testis single-cell dataset. Left, schematic of testis. Middle, embedding colored by annotated testis cell types. Right, feature plot showing Crz (green), SP (red) and β2-tubulin (blue) expression, with β2-tubulin marking spermatogenic populations and Crz detected only in a small subset of cells.

(C) Strip/dot plot summarizing normalized Crz expression across selected testis cell clusters, illustrating sparse Crz expression without broad enrichment in a major lineage. The y-axis signifies the expression level.

634 ## Discussion

635 Our study unveils a novel function of CRZ in an endogenous female signaling
636 pathway that modulates the post-mating reproductive behavior and physiology
637 (collectively PMR) in BPHs. It is, thus, the first report linking CRZ to a PMR in insects.
638 In contrast to SP and DUP99B in *D. melanogaster* [5,18], HP-1 in *Aedes aegypti* [15] and
639 maccessin (macc) recently identified in BPHs [24], CRZ is not produced in the MAG,
640 and thus not transferred from males during copulation. Instead, it is acting as an
641 endogenous peptide derived from neuroendocrine cells in the female brain. Moreover,
642 this CRZ-mediated endogenous modulation in females is seen also in *D.*
643 *melanogaster.* When *Crz* is knocked down or knocked out in flies, mated females
644 likewise exhibit an altered PMR.

645 Focusing on the endogenous CRZ signaling in female BPHs, our main findings
646 using mutants and RNAi of both *Crz* and *CrzR*, demonstrate that CRZ signaling
647 decreases the female responsiveness to courting males, especially in already mated
648 females. Also, oviposition in mated BPHs is increased by CRZ signaling. CRZ
649 immunolabeling revealed a small set of neurons in the brain and subesophageal
650 ganglion and no CRZ was detected in reproductive organs. Thus, the likely source of
651 CRZ affecting the PMR is the CRZ-producing neuroendocrine cells in the brain. In
652 insects studied so far (including other hemipterans), there are at least three pairs of
653 CRZ expressing lateral neurosecretory cells with axon terminations in the corpora
654 cardiaca [55,56], suggesting that in BPHs and *D. melanogaster* hormonal CRZ may
655 contribute to the modulation of the PMR. However local CRZ signaling in brain circuits
656 cannot be excluded since the CRZ neurons arborize extensively within the brain.

657 We found that the CRZ receptor, *CrzR*, is predominantly expressed in the female
658 reproductive tract in BPHs, more specifically in the lower tract including the
659 spermatheca and pouched gland, which are sites of sperm and seminal fluid storage.
660 Thus, in BPHs, CRZ may act to regulate the release of stored sperm and seminal fluid
661 in the female. This regulation would also gate the flow of male-derived factors that
662 induce and maintain the PMR, such as macc and ITPL-1. As mentioned, we cannot
663 exclude additional action of CRZ in neuronal circuits in the CNS that regulate female

sexual arousal and reproductive behavior, since our PCR data indicate expression of the *CrzR* also in the CNS. Additionally, the fat body of BPHs, express *CrzR*, similar to *D. melanogaster* [57], possibly suggesting a role of CRZ in post-mating metabolism.

The brain CRZ neurons of BPHs are likely to be activated by sensory signals from the female reproductive tract upon copulation and hence release CRZ into the circulation (and maybe within the brain). In *D. melanogaster,* sensory neurons in the reproductive tract are activated by SP (via the SP receptor), and signal via a chain of ascending axons of the VNC to sex-specific neurons in the brain to induce the PMR switch in behavior and physiology [7,38,40,58]. Thus, in *D. melanogaster,* these sex-specific circuits may also activate the CRZ neurons. Possibly similar sensory and sex-specific neurons exist in BPHs and respond either to mechanical stimuli or factors in the seminal fluid leading to activation of CRZ neurons and other brain neurons that regulate the PMR.

The female PMR is complex in *D. melanogaster* and not only receptivity and oviposition are affected, but also feeding, metabolism, sleep patterns and aggression [5,16,18,19,59,60]. In BPHs only the receptivity (and associated rejection behavior) and oviposition have been analyzed in any detail. We found that the MAG-derived peptides transferred with the semen, macc and ITPL-1, only affected the receptivity [24], whereas we show here that CRZ affects also oviposition. Thus, we have identified three different peptides CRZ, macc and ITPL-1 that all influence the PMR in different ways, suggesting complex regulatory mechanisms also in BPHs.

It is interesting to note that CRZ is an evolutionarily conserved neuropeptide that has been found in most, but not all, insect species and it displays a wide array of functions [56,57,61,62]. The CRZ function varies across different insect species, but a common role seems to be in regulation of stress [62-64]. Other functions are for example: in the American cockroach, CRZ accelerates the heart rate [65], in locusts, it triggers the formation of pigments that darken the body color in gregarious insects [66], in the moth *Bombyx mori*, CRZ affects developmental speed and reduces the rate of silk spinning behavior [67]; in *D. melanogaster* larvae, CRZ regulates molting motor behavior [68] and growth [69]; in adult *D. melanogaster* CRZ regulates stress responses, food intake and

metabolism [57,70], and protein food preference [12], as well as sperm ejection and mating duration in males [45]; and in social ants, it regulates the social hierarchy and inhibits egg-laying in the queen [48]. Finally, a recent study found that CRZ mediates a diapause-induced suppression of reproduction in female bean bugs [71]. To all these functions can now be added the role of CRZ in reproductive behavior and physiology of female BPHs and *D. melanogaster*. Finally, building on the role of CRZ in metabolism shown in *D. melanogaster* [57], it is possible that CRZ also regulates post-mating metabolism in female BPHs and flies. Thus, there may be a link between CRZ and the altered feeding and metabolism commonly seen in mated female insects that ensures optimal egg development[5,9,16].

CRZ and the vertebrate peptide gonadotropin-releasing hormone (GnRH) are paralogs that arose via an ancient gene duplication, and act on evolutionarily conserved receptors[72,73]. *Bona fide* GnRHs have not been found in arthropods and the CRZ peptide has been lost in the vertebrate lineage, but the cephalochordate (lancelet) *Branchiostoma floridae* does have peptides of both types[73]. In vertebrates, including humans, GnRH regulates female reproduction (specifically sexual maturation)[74,75]. We have shown here that CRZ regulates reproductive behavior and physiology in females of *D. melanogaster* and previous reports demonstrated a role in female fecundity[76] and a reproductive function also in males of this species[45]. Thus, CRZ and GnRH share a major function that may be ancient, although CRZ signaling in insects has evolved to also regulate stress responses, metabolism and development[57,62,77] .

Some outstanding questions remain with respect to mechanisms of CRZ signaling in the female PMR. The inputs triggering release of hormonal CRZ at mating are not known in BPHs or flies. This can probably be best investigated in *Drosophila* where brain neurons that are targets of the sex peptide receptor expressing neurons in the oviduct have been identified[58], and synaptic inputs to CRZ producing brain neurons have been described[78]. Once candidate interneurons interacting with the CRZ neurons have been identified, genetic manipulations of these neurons may unveil how mating triggers endogenous CRZ signaling and the PMR. Another aspect

of CRZ signaling that merits further study in *Drosophila* is the link between CRZ and the post-mating change in feeding and metabolism. At present it is not known whether also BPHs change their feeding and metabolism after mating, but would be valuable to investigate to determine to what extent the PMR in the two insects are similar. Finally, since BPHs are a major rice pest, it may be useful to further investigate the regulation of the PMR to design novel strategies for control their reproduction.

Table legend:

Table 1. Primers used in this study

Primer name	Sequence (5'-3')	Purpose
NlCrz-F	ACCGCATCAGGACGACAATA	Gene clone
NlCrz-R	ACCATAGCTGTTGAGCTACAAAT	
NlCrz-RNAi-F	TAATACGACTCACTATAGGGGCTAGTGTTGCAATGCTGTTG	*dsNlCrz* synthesis
NlCrz-RNAi-R	TAATACGACTCACTATAGGGGCTGTTGAGCGTTAGACTGT	
QNlCrz-F	AGACAGTGACCACAGCTCAA	qRT-PCR for NlCrz
QNlCrz-R	GAGTACTGGAACGTCTGTGC	
NlCrz-sgRNA-F1	TAATACGACTCACTATAGGCACAGGAGTGATGCAGAC	sgRNA synthesis for NlCrz knock-out
NlCrz-sgRNA-R1	TTCTAGCTCTAAAACGTCTGCATCACTCCTGTGCC	
NlCrz-sgRNA-F2	TAATACGACTCACTATAGCTACTAGTGCTGGGCTGCA	sgRNA synthesis for NlCrz knock-out
NlCrz-sgRNA-R2	TTCTAGCTCTAAAACTGCAGCCCAGCACTAGTAGC	
NlCrz Check F	ACCATAGCTGTTGAGCTACAAAT	To analyze NlCrz mutant
NlCrz Check R	TGCAATGCTGTTGTCGCGAC	
NlCrzR-F	AATCAGGCGATGAACCTCAGTT	Gene clone
NlCrzR-R	ACGCAGTTCTATGACGTGAGG	
NlCrzR-RNAi-F	TAATACGACTCACTATAGGGCGCCGTCTACACACTCATCT	*dsNlCrzR* synthesis
NlCrzR-RNAi-R	TAATACGACTCACTATAGGGCTACCAGCTTCGTACAGCGT	
QNlCrzR-F1	CTGGTGCTAATAGGGCTGGA	qRT-PCR for NlCrzR
QNlCrzR-R1	TCCGGTGTACAGTTGCTCTT	
QNlCrzR-F2	TGCTCACCATCGCCTCTATC	qRT-PCR for NlCrzR
QNlCrzR-R2	TGCCATGGTTCCGTGTAGAA	
NlCrzR-F1	CCCACTAGCCAGCAACCATT	RT-PCR for NlCrzR
NlCrzR-R1	TCCTCCACAAATGGTCCACG	
NlCrzR-sgRNA-F1	TAATACGACTCACTATAGGCACGCACTCGAGCTGCCT	sgRNA synthesis for NlCrzR knock-out
NlCrzR-sgRNA-R1	TTCTAGCTCTAAAACAGGCAGCTCGAGTGCGTGCC	
NlCrzR-sgRNA-F2	TAATACGACTCACTATAGGCGATGGTGAGCAGGTTGC	sgRNA synthesis for NlCrzR knock-out
NlCrzR-sgRNA-R2	TTCTAGCTCTAAAACGCAACCTGCTCACCATCGCC	
NlCrzR Check-F	GGCAGCAACCTGAGCCACCC	To analyze NlCrzR mutant

NlCrzR Check-R	GTCTTACCAGCGACCCAAGC	
QNlvg-F	GTGGCTCGTTCAAGGTTATGG	qRT-PCR for Nlvitellogenin
QNlvg-R	GCAATCTCTGGGTGCTGTTG	
QNlvgR-F	AGGCAGCCACACAGATAACCGC	qRT-PCR for Nlvitellogenin receptor
QNlvgR-R	AGCCGCTCGCTCCAGAACATT	
QNl53903-R	GTCCACCGAACTTTTCCTGG	
QNl Macc-F	TCTTTGGAAGTGGTGATTCCATCT	qRT-PCR for NlMacc
QNl macc-R	TGTCTACTTCACATACATGTGGCT	
QNl itpl-1-F	GATCAGATTCAATTCACATTCCTC	qRT-PCR for Nlitpl-1
QNl itpl-1-R	AGATTGTAGCAGTCCTCGCATA	

736 Key resources table

REAGENT or RESOURCE	Source or reference	Identifiers
Antibodies		
Goat anti-Rabbit Alexa 488	Invitrogen	Cat#A11008; RRID: AB_143165
Goat anti-mouse Alexa 488	Invitrogen	Cat#A28175; RRID: AB_2536161
Goat anti-mouse Alexa 555	Invitrogen	Cat# A21428; RRID: AB_2535849
Anti-CRZ	Gift from Prof. Jan A. Veenstra	
Chemicals, Peptides, and Recombinant Proteins		
4% PFA	Leagene	Cat# DF0134
DAPI	Solarbio	Cat# C0060
PBS	Solarbio	Cat# P1022
ReadyProbes 2.5% Normal Goat Serum	Invitrogen	Cat# R37624
Experimental Models: Organisms/Strains		
Canton-S	Bloomington Drosophila Stock Center	64349
Crz^{attp}	Rao and Deng et al., 2019	BDSC: 84487
Crz-GAL4	Bloomington Drosophila Stock Center	51976
Crz-RNAi	Tsinghua Fly Center	THU2139
Software and Algorithms		
FIJI		https://doi.org/10.1038/nmeth.2019
Prism 9	GraphPad	RRID: SCR_002798
Photoshop	Adobe	RRID: SCR_014199
Illustrator	Adobe	RRID: SCR_010279
ZEN	Zeiss	N/A
Motic Images Plus3.0	Motic	N/A
Motic Images Devices	Motic	N/A
Other		
Egg-laying device	Gou et al., 2016	N/A
Anatomical tweezers	Dumont	Cat# 0209-5-PO

737

738

739 **Method details**

740 **Experiment insects**

741 All the brown planthoppers used in this research were collected from Hangzhou,
742 Zhejiang Province in 1995. The insects were kept indoors on fresh rice seedlings
743 (Taichung Native 1, TN1) in a growth chamber at 27 ± 1 °C and 70 ± 10% relative humidity,
744 under a 16 h:8 h (Light: Dark) photoperiod [79].

745 All *D. melanogaster* stocks were raised in standard cornmeal–molasses–agar
746 medium maintained at 25° C, 60% humidity, and under 12 hr:12 hr light:dark conditions.
747 We used Canton s flies as the wild-type strain. The relevant information about fruit flies
748 used in the experiments are shown in key resources table.

749

750 **Male accessory gland protein extraction of *Nilaparvata lugens***

751 Protein extraction was performed as described previously[24]. Male accessory glands
752 (MAGs) were dissected from 3–5-day-old virgin males in phosphate buffer (pH 7.2) under
753 a stereomicroscope. For protein extraction, approximately 300 MAGs were collected,
754 immediately frozen, and stored at −80 °C until use. Frozen MAGs were pre-ground in
755 liquid nitrogen and then lysed in 500 μL protein cracking buffer (100 mM NH_4HCO_3, 8 M
756 urea, 0.2% SDS, pH 8.0) with thorough homogenization. Lysates were centrifuged at
757 12,000 × g for 15 min at 4 °C, and the supernatants were collected as soluble protein
758 extracts. Protein concentration was determined using a Bradford colorimetric assay (BSA
759 as the standard; absorbance at 595 nm). Protein integrity and quality were assessed by
760 SDS–PAGE. Protein extracts were stored at −80°C until next step experiment.

761

762 **Behavior assays of *Nilaparvata lugens***

763 *Mating and receptivity*

764 All BPHs were raised in incubators with a 16 h:8 h dark:light cycle. Unmated female and
765 male BPHs were collected within 12 hours of emergence. For RNAi or neuropeptide
766 injection treatment, the protocol is shown in Figure 1A and Figure 1D. The mating
767 behavior (or female receptivity behavior) test in this study usually conducted the first
768 mating between 3 and 5 days after emergence. The mating experiment was completed in

a plastic tube (2.5cm in diameter and 10cm in height). Fresh rice seedlings of appropriate length were placed in each tube, and then a female and a male BPH was added. The mating conditions and other reproductive behavior parameters during this period were observed in a constant temperature room at 25°C for 30min, and the males were taken out after 30 min. In *N. lugens*, mating induces a transient suppression of female receptivity that is not permanent; females typically start to regain remating willingness 72 h after the first mating, as documented in our previous study[24]. This temporal window guided the design of our remating assays, in which females were paired with naive males at 48 h, post-initial mating to capture both the suppressed and recovered phases of receptivity. For the experiment requiring a second mating, females successfully mated for the first time were retained. After 48 hours, wild-type males were put in for the re-mating test. The males in all secondary mating experiments were wild type. The monitoring time for each mating behavior was 30 minutes; the receptivity rate refers to the proportion of successful matings of female individuals within the 30-minute measurement period.

Egg laying

After completing the first mating, the male is sucked out and a sufficient number of rice seedlings are added to the tube, and the female is retained to lay eggs in the tube. After 72 hours, the spawning female is transferred out of the tube. After the eggs have matured, about 4-5 days later, we used tweezers to gently manipulate the rice seedlings and counted the number of fertilized eggs produced by the females. Note that 4 to 5 days after the egg is produced, the successfully fertilized egg will display red eye-spots. Oviposition assay protocol: For quantitative assessment of post-mating responses, egg-laying activity was monitored over a 72-hour observation window following verified initial copulation. To eliminate confounding effects from sequential mating trials, experimental subjects undergoing oviposition measurement were permanently excluded from subsequent re-mating evaluations.

To assess oviposition in females injected with CRZ peptide, virgin or mated female BPHs (3–5 days post-emergence) were transferred into plastic tubes containing sufficient rice seedlings 6 h after recovery from peptide injection. Females were allowed to oviposit for

24 h and were then removed. Eggs were subsequently counted by gently dissecting the rice seedlings with forceps.

Behavior assays of *D. melanogaster*

Mating and re-mating：During the receptivity assessment, all experimental fruit flies were virgin flies that emerged within 12 hours in a 20°C incubator in a 12 h:12 h dark:light cycle. After collection, they were kept at 25°C incubator in a 12 h:12 h dark:light cycle for 4 days before behavioral testing. Receptivity behavior measurement：a perforated plate was placed on top of a non-perforated plate. Male fruit flies were briefly anesthetized on ice and gently transferred into the holes of the perforated plate, with one male per hole. Once the male transfer was completed, a plastic film was gently placed over the perforated plate, followed by covering it with another perforated plate. Then, the virgin female fruit fly, also anesthetized on ice, was placed in each hole. After the transfer was completed, a non-perforated plate was placed on top. This setup was then transferred to a 25°C incubator to acclimate for 30 minutes. The plastic film separating the male and female flies was quickly removed, and video recording began for 30 minutes. The recorded videos were analyzed to calculate the acceptance rate of the females. Successful mating females were collected and individually transferred into plastic tubes containing sufficient artificial food for fruit flies to lay eggs. After 24 hours of laying eggs, the female flies were transferred to a new finger-shaped tube with ample artificial feed for another 24 hours of laying. After 48 hours, these egg-laying females were subjected to a secondary mating assessment with wild-type, unmated males, using the same method as described above, to evaluate the acceptance rate during the second mating process. Additionally, the number of eggs laid by each female during the 48 hours was recorded.

Egg laying for mated females：First, collect virgin female fruit flies that eclosion within 12 hours at 20°C incubator in a 12 h:12 h dark:light cycle and then keep them in a 25°C incubator in a 12 h:12 h dark:light cycle for 4 days. After that, unmated males of the wild type and virgin females were mixed 1:1.5 times. 24 hours after full mating, female flies were lightly anesthetized with ice and transferred to plastic vials containing enough artificial fruit fly food for them to lay eggs for 24 hours. After 24 hours, the flies were

829 transferred again to a new bottle full of artificial food for another 24 hours of egg laying.
830 The number of eggs in each vial is calculated under a microscope, and the total number of
831 eggs in the two vials of each female fruit fly represents the egg-laying capacity of that
832 individual.
833
834 **Developmental duration statistics**
835 Nymphs of BPHs that hatched synchronously from distinct genotypes were collected and
836 reared in plastic cups containing fresh rice seedlings; the seedlings were replaced
837 regularly to maintain optimal conditions. From the day the nymphs reached the fifth instar,
838 cups were inspected daily for adult emergence, and the number of newly emerged adults
839 was recorded. After all surviving individuals had completed eclosion, the total
840 nymph-to-adult developmental duration was calculated.
841
842 **BPHs survival rate statistics**
843 For neuropeptide injection: After 4-day emergence, virgin BPHs were injected with CRZ
844 neuropeptide or scrambled CRZ, and after 6 hours of recovery, these insects were placed
845 into a plastic tube with sufficient quantity of rice seedlings. Survival was monitored every
846 24 hours until all specimens were dead.
847 For mutant: Wild-type and mutant BPHs adults that eclosed on the same day were
848 individually confined in plastic tubes, each supplied with ample fresh rice seedlings and
849 water renewed regularly to ensure optimal living and nutritional conditions. The number of
850 surviving individuals of each genotype was recorded every 24 h until all had died, and
851 survival curves were generated from these data.
852
853 **Neuropeptide synthesis and injection.**
854 Corazonin (CRZ) and scrambled CRZ (sCRZ) were synthesized by Genscript Co. Ltd
855 (Nanjing, China). Peptide masses were confirmed by Mass spectrometry and the amount
856 of peptide was quantified by amino acid analysis. The amino acid sequences of the
857 peptides used in this study are: *N. lugens* corazonin: pQTFQYSRGWNamide; scrambled
858 corazonin: pQSRYTTFGQWTNamide. On the fourth day after adult emergence, virgin

859 female BPHs were injected with different concentrations of synthetic CRZ peptide and
860 control scrambled peptide. The scrambled peptide control was used to monitor for
861 potential non-specific effects on behavior due to the process of injection. Each mg peptide
862 was dissolved in 100 μl DMSO solution (Acmec, #D54264), and then diluted to 1.5 mM,
863 0.15 mM, 0.015 mM and 0.0015 mM with 1×PBS as solvent. The BPHs were anesthetized
864 with CO_2 for about 30 seconds and placed abdomen up on 2% agarose (Solarbia, #A8201)
865 plate and 50 nl neuropeptide solution injected into each female. Six hours after
866 neuropeptide injection the insects were used for behavior assay.
867

868 **Gene cloning and sequence analysis**

869 We used the NCBI database with BLAST programs to carry out sequence alignment and
870 analysis. Then we predicted Open Reading Frames (ORFs) with EditSeq. The primers
871 were designed by Primer designing tool in NCBI. Total RNA Extraction was using the
872 TRIzol reagent (Invitrogen, Carlsbad, CA, USA) according to the manufacturer's
873 instructions. The cDNA template used for cloning was synthesized using the Biotech
874 M-MLV reverse transcription kit and the synthesized cDNA template was stored at -20˚C.
875 The transmembrane segments and topology of proteins were predicted by TMHMM v2.0
876 (http://www.cbs.dtu.dk/services/TMHMM-2.0/) [80]. Multiple alignments of the complete
877 amino acid sequences were performed with Clustal Omega
878 (http://www.ebi.ac.uk/Tools/msa/clustalo).
879

880 **qRT-PCR for spatial expression pattern and RNAi efficiency**

881 The nervous system (NS), fat body (Fb), digestive system (DS), epidermis (EP), male
882 reproductive organs (MRO) and female reproductive organs (FRO) from 3-5 days old
883 adults were dissected in 1×PBS, to determine the tissue-specific expression pattern. With
884 the exception of the reproductive system, the rest of the tissue comes from both sexes
885 equally. The adult BPHs were placed on ice under slight anesthesia and dissected under
886 a stereoscopic microscope (ZEISS). At least 50 individuals were dissected as one sample
887 for tissue-specific analysis with three replicates. All tissues were quickly transferred to
888 Trizol (Invitrogen, Carlsbad, CA, USA) solution at 0° C after dissection.

889 For RNAi efficiency testing, we collected the whole bodies of BPHs and transferred to a
890 1.5 mL EP tube containing Trizol reagent. Total RNA extraction was using Trizol reagent
891 (Invitrogen, Carlsbad, CA, USA) according to the manufacturer's instructions. The cDNA
892 template used for cloning was synthesized using the Biotech M-MLV reverse transcription
893 kit and the synthesized cDNA template was stored at -20˚C.
894 Real-time qPCRs of the various samples used the UltraSYBR Mixture (with ROX) Kit
895 (CWBIO, Beijing, China). The PCR was performed in 20μl reaction including 2 μl of
896 10-fold diluted cDNA, 1 μl of each primer (10 μM), 10μl 2 × UltraSYBR Mixture, and 6 μl
897 RNase-free water. The PCR conditions used were as follows: initial incubation at 95˚C for
898 10 min, followed by 40 cycles of 95˚C for 10 s and 60˚C for 45 s. *N. lugens* 18S rRNA and
899 actin were used as an internal control (primers listed in Table1). Relative quantification
900 was performed via the comparative $2^{-\Delta\Delta CT}$ method [81].
901
902 **RNAi and RNAi efficiency determination**
903 For lab-synthesized dsRNA, *gfp*, Nl*CrzR* and Nl*Crz* were amplified by PCR using specific
904 primers conjugated with the T7 RNA polymerase promoter (primers listed in Table1).
905 dsRNA was synthesized by the MEGAscript T7 transcription kit (Ambion, Austin, TX, USA)
906 according to the manufacturer's instructions. Finally, the quality and size of the dsRNA
907 products were verified by 1% agarose gel electrophoresis and the Nanodrop 1000
908 spectrophotometer and kept at -70˚C until use.
909 3-5 days old virgin female BPHs were used for injection of 50nl of 5 μg/μl dsRNA per
910 insect. Injection of an equal volume of ds*gfp* was used as negative control. After 48 hours,
911 the insects were used behavior assays and gene relative expression analysis.
912
913 **Neuropeptide injection after RNAi**
914 48 hours after the ds*CrzR* injection, each insect was injected again with 10 ng of peptide
915 dissolved in 50 nL of 1 × PBS balanced salt solution. Recovery was for six hours after
916 injection. These insects were used for behavior assays. RNAi efficiency was examined by
917 qPCR using a pool of ten individuals 48 hours after dsRNA injections.
918

919 **In vitro synthesis of sgRNA and Cas9 mRNA**

920 The single guide RNA (sgRNA) was designed as previously reported [82]. Briefly, sgRNA
921 was designed by manually searching genomic sequence around the region of the *Crz* and
922 *CrzR* exon for the sequences corresponding to 5'-$N_{17\text{-}20}$NGG-3', where NGG is the
923 protospacer-adjacent motif (PAM) of SpCas9 and N is any nucleotide. For in vitro
924 transcription of sgRNA, were synthesized in vitro using the GeneArt™Precision gRNA
925 Synthesis Kit (Thermo Fisher Scientific, Vilnius, Lithuania) according to the instructions of
926 manufacturer. The Cas9 protein (TrueCut™Cas9 Protein v2, Cat. NO. A36497) was
927 purchased from Thermo Fisher Scientific (Shanghai, China).

928

929 **Embryo microinjection, crossing and genotyping**

930 The embryonic injection was performed as previously reported [83]. The female BPHs,
931 which had been mated for 3-6 days after emergence, were selected to lay eggs. After 30
932 minutes, the embryos were transferred onto double-sided tape attached to a microscope
933 slide along the long edge by gently pressing the slide onto the dorsal surface of embryos.
934 A few drops of halocarbon oil 700 was added to these eggs. About 0.5–1 nL mixture of
935 Cas9 protein (200 ng/μL) and sgRNA (100 ng/μL) was injected into each egg using a
936 FemtoJet and Inject Man NI 2 microinjection system (Eppendorf, Germany). After the
937 injection, the eggs were placed in Petri dishes covered with moist filter paper, and the
938 Petri dishes were placed in plant growth chamber at 27±1 °C, 70±10% RH for hatching.
939 These eggs hatched into G0 generations.

940

941 **Crossing and genotyping**

942 To establish homozygous mutants of *Nilaparvata lugens* through CRISPR-mediated gene
943 editing, newly emerged G0 adults were outcrossed with wild-type counterparts to
944 generate G1 progeny. Following successful mating and oviposition, genomic DNA was
945 extracted from G0 adults for mutation screening. The target region surrounding NlCrzR
946 was amplified by PCR using specific primers NlCrzR-check-F and NlCrzR-check-R
947 (primer sequences listed in Table 1), followed by Sanger sequencing to identify G0
948 individuals carrying mutations.

949 Progeny (G1) from mutation-positive G0 parents were maintained through sibling crosses
950 to establish G2 populations. Subsequent genotyping via Sanger sequencing was
951 performed on G1 individuals to select breeding pairs where both male and female parents
952 carried heterozygous mutations. The resulting G2 offspring from these validated pairs
953 were then subjected to intercrossing to ultimately generate homozygous mutant lines.
954 After homozygous mutant lines were established, virgin homozygous mutant females
955 were paired individually with virgin wild-type males. Following successful copulation,
956 inseminated females were transferred to fresh rice seedlings for oviposition, and fertilized
957 eggs were allowed to hatch. Hatched nymphs were continuously reared on fresh rice
958 seedlings until the fifth instar. Rice seedlings were replaced every 12 hours, and newly
959 emerged adults were collected and sex-separated for subsequent behavioral assays.
960

961 **Quantitative RT-PCR**

962 The first-strand cDNA was synthesized with HiScript II Q RT SuperMix for qPCR (+gDNA
963 wiper) kit (Vazyme, Nanjing, China) using an oligo (dT)18 primer and 500 ng total RNA
964 template in a 10 μl reaction, following the instructions. Real-time qPCRs in the various
965 samples used the UltraSYBR Mixture (with ROX) Kit (CWBIO, Beijing, China). The PCR
966 was performed in 20 μl reaction including 4 μl of 10-fold diluted cDNA, 1 μl of each primer
967 (10 μM), 10 μl 2 × UltraSYBR Mixture, and 6 μl RNase-free water. The PCR conditions
968 used were as follows: initial incubation at 95˚C for 10 min, followed by 40 cycles of 95˚C
969 for 10 s and 60˚C for 45 s. *N. lugens* 18S rRNA or *D. melanogaster* rp49 were used as an
970 internal control (Table 1). Relative quantification was performed via the comparative
971 $2^{-\Delta\Delta CT}$ method (Livak, K. J,2001).
972

973 **Immunohistochemistry**

974 Adult BPHs, 3-5 days old, were dissected under 1x phosphate-buffered saline (PBS; pH
975 7.4) in Schneider's insect medium (S2). We dissected the brain, ventral nerve cord and
976 reproductive system of the BPHs. These tissues were fixed in 4% paraformaldehyde in
977 PBS for 30 min at room temperature. After extensive washing with PTX (0.5% Triton X100,
978 0.5% bovine serum albumin in PBS), blocked in 3% normal goat serum. Then, the tissues

979 were incubated in Anti - CRZ for 12 hours at 4℃ and in secondary antibody for 12 h at
980 4℃. Primary antibodies used were: rabbit anti - CRZ (1:1000, Anti - CRZ was gift from Jan
981 A. Veenstra), mouse anti-Bruchpilot (1:1000, Developmental Studies Hybridoma Bank
982 nc82). Secondary antibodies used: donkey anti-rabbit IgG conjugated to Alexa 488 (1:500,
983 R37118, Thermo Fisher Scientific) and donkey anti-mouse IgG conjugated to Alexa Alexa
984 555 (1:500, R37115, Thermo Fisher Scientific). The samples were mounted in
985 Vectorshield (Vector Laboratory). Images were acquired with Zeiss LSM 700 confocal
986 microscopes, and were processed with Image J software. All antibodies were diluted in
987 PTX solution. The primary antibody was diluted at a ratio of 1:1000, while the secondary
988 antibody was diluted at a ratio of 1:500.

989 Adult female *D. melanogaster*, 3-5 days old, were dissected under 1 x
990 phosphate-buffered saline (PBS; pH 7.4) in Schneider's insect medium (S2). We
991 dissected the brain, ventral nerve cord and reproductive system. These tissues were fixed
992 in 4% paraformaldehyde in PBS for 30 min at room temperature. After extensive washing
993 with PTX (0.5% Triton X100, 0.5% bovine serum albumin in PBS), blocked in 3% normal
994 goat serum. Then, the tissues were incubated in Anti - CRZ and Anti - nc82 for 12 hours at
995 4℃ and in secondary antibody for 12 h at 4℃. Primary antibodies used were: rabbit
996 anti-CRZ (1:1000, A11122, Provided by Jan A. Veenstra). Secondary antibodies used:
997 donkey anti-rabbit IgG conjugated to Alexa 488 and anti-mouse IgG conjugated to Alexa
998 555 (R37118, Thermo Fisher Scientific). The samples were mounted in Vectorshield
999 (Vector Laboratory). Images were acquired with Zeiss LSM 700 confocal microscopes,
1000 and were processed with Image J software. All antibodies were diluted in PTX solution.

1001

1002 **Fluorscent in situ hybridization (FISH)**

1003 FISH was performed as previously reported by Yan et al. [84]. Briefly, the reproductive
1004 system of the female BPH dissection was performed under 1x Phosphate Buffered Saline
1005 (PBS) supplemented with a protease and phosphatase inhibitor cocktail (Shyuanye,
1006 #R40012) on a clean, clear rubber pad using two fine forceps (Dumont, #0108-5-po).
1007 Dissected tissues were fixed using 4% paraformaldehyde (PFA) (Shyuanye, #22039)
1008 diluted in 1 x PBS with 0.1% Tween20 (0.1% PBST) at room temperature (RT) for 20 min

on a shaker. Fixed tissues were washed three times with 0.1% PBST for 15 min each on a shaker. The tissues were dehydrated in 25%, 50%, 90% and 100% methanol, and then rehydrated in reverse order, performed at room temperature for 10 minutes at a time. The tissue was then washed twice with 0.1% PBST and shaken for 5 minutes. A post fixation was performed by incubating the tissue in 4% PFA in 1 x PBS on a shaker for 20 minutes, followed by two washes with PBST for 5 minutes each while shaking. The tissue was permeabilized with proteinase K (10 μg/ml) at room temperature for 2 minutes. After incubation, the tissue was washed with 0.1% PBST for 5 minutes while shaking. The PBST was removed, and pre-hybridization solution (Boster, #AR0152) was applied at 55°C for approximately 2 hours. The DIG probes were denatured in a metal bath at 80°C for 5 minutes and then immediately placed on ice. The denatured DIG-labeled probes were added to the hybridization solution, and hybridization was carried out overnight at 55°C. Then, the hybridized tissue was washed twice at 55°C for 40 minutes with warm pre-hybridization solution, followed by four washes at room temperature with 0.1% PBST for 10 minutes each. The detection of the DIG-labeled probes was performed using an anti-DIG conjugated fluorescent antibody (1:100 dilution, Jackson, #200-542-156), incubated at room temperature in 0.1% PBST for 2 hours, followed by three washes with 0.1% PBST. Finally, the tissue was mounted in mounting medium and imaged using a Zeiss confocal microscope.

Quantification and statistical analysis

All graphs were generated using Prism 9 software (GraphPad Software, La Jolla, CA). Data presented in this study were first verified for normal distribution by D'Agostino– Pearson normality test. If normally distributed, Student's *t* test was used for pairwise comparisons, and one-way ANOVA and chi-square was used for comparisons among multiple groups. If not normally distributed, Mann–Whitney test was used for pairwise comparisons, and Kruskal–Wallis test was used for comparisons among multiple groups, followed by Dunn's multiple comparisons. All data are presented as mean ± s.e.m.

Data availability statement: All of the RNA sequence data in this article have been

deposited in the China National Center for Bioinformation database and are accessible in PRJCA045433.

ACKNOWLEDGMENTS: We thank Dr. Jan A. Veenstra for providing CRZ antibody. This project was supported by National Key R&D Program of China (2022YFD1700200) to S.-F.W., the National Natural Science Foundation of China (No. 32472542) to S.-F.W..

References:

1. Do-Hyoung Kima , Y.-Hoon J., , Minsik Y., and , K.-Min L., and Young-Joon Kima,1 (2024). Long-term neuropeptide modulation of female sexual drive via the TRP channel in Drosophila melanogaster. Proceedings of the National Academy of Sciences. 10.1073/pnas.
2. Sun, M., Ma, M., Deng, B., Li, N., Peng, Q., and Pan, Y. (2023). A neural pathway underlying hunger modulation of sexual receptivity in Drosophila females. Cell Rep *42*. 10.1016/j.celrep.2023.113243.
3. Wang, F., Wang, K., Forknall, N., Parekh, R., and Dickson, B.J. (2020). Circuit and Behavioral Mechanisms of Sexual Rejection by Drosophila Females. Current biology : CB. 10.1016/j.cub.2020.07.083.
4. Wang, K., Wang, F., Forknall, N., Yang, T., Patrick, C., Parekh, R., and Dickson, B.J. (2021). Neural circuit mechanisms of sexual receptivity in Drosophila females. Nature *589*, 577-581. 10.1038/s41586-020-2972-7.
5. Kubli, E. (2003). Sex-peptides: seminal peptides of the Drosophila male. Cell Mol Life Sci *60*, 1689-1704. 10.1007/s00018-003-3052.
6. Yapici, N., Kim, Y.J., Ribeiro, C., and Dickson, B.J. (2008). A receptor that mediates the post-mating switch in Drosophila reproductive behaviour. Nature *451*, 33-37. 10.1038/nature06483.
7. Yang, C.H., Rumpf, S., Xiang, Y., Gordon, M.D., Song, W., Jan, L.Y., and Jan, Y.N. (2009). Control of the postmating behavioral switch in Drosophila females by internal sensory neurons. Neuron *61*, 519-526. 10.1016/j.neuron.2008.12.021.
8. Rezaval, C., Pavlou, H.J., Dornan, A.J., Chan, Y.B., Kravitz, E.A., and Goodwin, S.F. (2012). Neural circuitry underlying Drosophila female postmating behavioral responses. Current biology : CB *22*, 1155-1165. 10.1016/j.cub.2012.04.062.
9. Camus, M.F., Huang, C.C., Reuter, M., and Fowler, K. (2018). Dietary choices are influenced by genotype, mating status, and sex in Drosophila melanogaster. Ecol Evol *8*, 5385-5393. 10.1002/ece3.4055.
10. Craig, G.B., Jr. (1967). Mosquitoes: female monogamy induced by male accessory gland substance. Science *156*, 1499-1501. 10.1126/science.156.3781.1499.
11. Judson, C.L. (1967). Feeding and oviposition behavior in the mosquito Aedes aegypti (L.). I. Preliminary studies of physiological control mechanisms. Biol Bull *133*, 369-378. 10.2307/1539832.
12. Liu, C., Tian, N., Chang, P., and Zhang, W. (2024). Mating reconciles fitness and fecundity by switching diet preference in flies. Nature communications *15*, 9912. 10.1038/s41467-024-54369-w.
13. Liu, H., and Kubli, E. (2003). Sex-peptide is the molecular basis of the sperm effect in Drosophila melanogaster. Proceedings of the National Academy of Sciences of the United States of America *100*, 9929-9933. 10.1073/pnas.1631700100.
14. Chapman, T., Bangham, J., Vinti, G., Seifried, B., Lung, O., Wolfner, M.F., Smith, H.K., and Partridge, L. (2003). The sex peptide of Drosophila melanogaster: Female post-mating responses analyzed by using RNA interference. Proceedings of the National Academy of Sciences of the United States of America *100*, 9923-9928. 10.1073/pnas.1631635100.

1088 15. Duvall, L.B., Basrur, N.S., Molina, H., McMeniman, C.J., and Vosshall, L.B. (2017). A Peptide
1089 Signaling System that Rapidly Enforces Paternity in the Aedes aegypti Mosquito. Current
1090 Biology *27*, 3734-3742.e3735. 10.1016/j.cub.2017.10.074.
1091 16. Wolfner, M.F. (2002). The gifts that keep on giving: physiological functions and evolutionary
1092 dynamics of male seminal proteins in Drosophila. Heredity *88*, 85-93.
1093 10.1038/sj.hdy.6800017.
1094 17. Gorter, J.A., Jagadeesh, S., Gahr, C., Boonekamp, J.J., Levine, J.D., and Billeter, J.C. (2016). The
1095 nutritional and hedonic value of food modulate sexual receptivity in Drosophila melanogaster
1096 females. Sci Rep *6*, 19441. 10.1038/srep19441.
1097 18. Chen, P.S., Stumm-Zollinger, E., Aigaki, T., Balmer, J., Bienz, M., and Böhlen, P. (1988). A male
1098 accessory gland peptide that regulates reproductive behavior of female D. melanogaster. Cell
1099 *54*, 291-298. https://doi.org/10.1016/0092-8674(88)90192-4.
1100 19. Ellendersen, B.E., and von Philipsborn, A.C. (2017). Neuronal modulation of D. melanogaster
1101 sexual behaviour. Curr Opin Insect Sci *24*, 21-28. 10.1016/j.cois.2017.08.005.
1102 20. Klowden, M.J. (1999). The check is in the male: male mosquitoes affect female physiology
1103 and behavior. J Am Mosq Control Assoc *15*, 213-220.
1104 21. Manning, A. (1962). A Sperm Factor Affecting the Receptivity of Drosophila Melanogaster
1105 Females. Nature *194*, 252-253. 10.1038/194252a0.
1106 22. McCall, P.J. (2000). The biology of mosquitoes: volume 2, sensory reception and behaviour. By
1107 A.N. Clements (Wallingford, CABI Publishing, 1999). 740 pp. Hard cover £95.00 (US$175.00).
1108 ISBN 0 85199 313 3. Bulletin of Entomological Research *90*, 99-99.
1109 10.1017/S0007485300000171.
1110 23. Lung, O., Tram, U., Finnerty, C.M., Eipper-Mains, M.A., Kalb, J.M., and Wolfner, M.F. (2002).
1111 The Drosophila melanogaster seminal fluid protein Acp62F is a protease inhibitor that is toxic
1112 upon ectopic expression. Genetics *160*, 211-224.
1113 24. Zhang, Y.J., Zhang, N., Bu, R.T., Nässel, D.R., Gao, C.F., and Wu, S.F. (2025). A novel male
1114 accessory gland peptide reduces female post-mating receptivity in the brown planthopper.
1115 Plos Genet *21*, e1011699. 10.1371/journal.pgen.1011699.
1116 25. Rines, I.G., Harrod, A.E., Hunt, J., Sadd, B.M., and Sakaluk, S.K. (2023). Disentangling effects of
1117 mating, nuptial gifts and accessory gland proteins on reproduction in female crickets. Anim
1118 Behav *196*, 1-7. https://doi.org/10.1016/j.anbehav.2022.11.008.
1119 26. Tripet, F., Touré, Y.T., Dolo, G., and Lanzaro, G.C. (2003). Frequency of multiple inseminations
1120 in field-collected Anopheles gambiae females revealed by DNA analysis of transferred sperm.
1121 Am J Trop Med Hyg *68*, 1-5.
1122 27. Klowden, M.J., and Russell, R.C. (2004). Mating affects egg maturation in Anopheles gambiae
1123 Giles (Diptera: Culicidae). J Vector Ecol *29*, 135-139.
1124 28. Naccarati, C., Audsley, N., Keen, J.N., Kim, J.H., Howell, G.J., Kim, Y.J., and Isaac, R.E. (2012).
1125 The host-seeking inhibitory peptide, Aea-HP-1, is made in the male accessory gland and
1126 transferred to the female during copulation. Peptides *34*, 150-157.
1127 10.1016/j.peptides.2011.10.027.
1128 29. Saudan, P., Hauck, K., Soller, M., Choffat, Y., Ottiger, M., Sporri, M., Ding, Z., Hess, D., Gehrig,
1129 P.M., Klauser, S., et al. (2002). Ductus ejaculatorius peptide 99B (DUP99B), a novel Drosophila
1130 melanogaster sex-peptide pheromone. Eur J Biochem *269*, 989-997.
1131 10.1046/j.0014-2956.2001.02733.x.

30. Herndon, L.A., and Wolfner, M.F. (1995). A Drosophila seminal fluid protein, Acp26Aa, stimulates egg laying in females for 1 day after mating. Proceedings of the National Academy of Sciences of the United States of America *92*, 10114-10118. 10.1073/pnas.92.22.10114.

31. Mackay, T.F.C., Ram, K.R., and Wolfner, M.F. (2007). Sustained Post-Mating Response in Drosophila melanogaster Requires Multiple Seminal Fluid Proteins. Plos Genet *3*. 10.1371/journal.pgen.0030238.

32. Heifetz, Y., Vandenberg, L.N., Cohn, H.I., and Wolfner, M.F. (2005). Two cleavage products of the Drosophila accessory gland protein ovulin can independently induce ovulation. Proceedings of the National Academy of Sciences of the United States of America *102*, 743-748. 10.1073/pnas.0407692102.

33. Desplan, C., Gligorov, D., Sitnik, J.L., Maeda, R.K., Wolfner, M.F., and Karch, F. (2013). A Novel Function for the Hox Gene Abd-B in the Male Accessory Gland Regulates the Long-Term Female Post-Mating Response in Drosophila. Plos Genet *9*. 10.1371/journal.pgen.1003395.

34. Hopkins, B.R., Angus-Henry, A., Kim, B.Y., Carlisle, J.A., Thompson, A., and Kopp, A. (2024). Decoupled evolution of the Sex Peptide gene family and Sex Peptide Receptor in Drosophilidae. Proceedings of the National Academy of Sciences of the United States of America *121*, e2312380120. 10.1073/pnas.2312380120.

35. Jang, Y.-H., Chae, H.-S., and Kim, Y.-J. (2017). Female-specific myoinhibitory peptide neurons regulate mating receptivity in Drosophila melanogaster. Nature communications *8*. 10.1038/s41467-017-01794-9.

36. Chen, J., Zhu, P., Jin, S., Zhang, Z., Jiang, S., Li, S., Liu, S., Peng, Q., and Pan, Y. (2025). A hormone-to-neuropeptide pathway inhibits sexual receptivity in immature Drosophila females. Proceedings of the National Academy of Sciences of the United States of America *122*, e2418481122. 10.1073/pnas.2418481122.

37. Avila, F.W., Sirot, L.K., LaFlamme, B.A., Rubinstein, C.D., and Wolfner, M.F. (2011). Insect seminal fluid proteins: identification and function. Annual review of entomology *56*, 21-40. 10.1146/annurev-ento-120709-144823.

38. Hasemeyer, M., Yapici, N., Heberlein, U., and Dickson, B.J. (2009). Sensory Neurons in the Drosophila Genital Tract Regulate Female Reproductive Behavior. Neuron *61*, 511-518. 10.1016/j.neuron.2009.01.009.

39. Rezával, C., Pavlou, H.J., Dornan, A.J., Chan, Y.B., Kravitz, E.A., and Goodwin, S.F. (2012). Neural circuitry underlying Drosophila female postmating behavioral responses. Current biology : CB *22*, 1155-1165. 10.1016/j.cub.2012.04.062.

40. Auer, T.O., and Benton, R. (2016). Sexual circuitry in Drosophila. Curr Opin Neurobiol *38*, 18-26. 10.1016/j.conb.2016.01.004.

41. Lin, P.X., Peng, Y.X., Xing, J.Y., Liu, Z.Y., Guo, F.R., Thia, J.A., Gao, C.F., and Wu, S.F. (2025). Cis-regulation of the CYP6CS1 gene and its role in mediating cross-resistance in a pymetrozine-resistant strain of Nilaparvata lugens. Insect biochemistry and molecular biology *177*, 104261. 10.1016/j.ibmb.2025.104261.

42. Wu, S.F., Zeng, B., Zheng, C., Mu, X.C., Zhang, Y., Hu, J., Zhang, S., Gao, C.F., and Shen, J.L. (2018). The evolution of insecticide resistance in the brown planthopper (Nilaparvata lugens Stål) of China in the period 2012-2016. Sci Rep *8*, 4586. 10.1038/s41598-018-22906-5.

43. Song, X.Y., Peng, Y.X., Wang, L.X., Ye, W.N., Pei, X.G., Zhang, Y.C., Zhang, S., Gao, C.F., and Wu, S.F. (2022). Monitoring, cross-resistance, inheritance, and fitness costs of brown

planthoppers, Nilaparvata lugens, resistance to pymetrozine in China. Pest management science *78*, 3980-3987. 10.1002/ps.7017.

44. Ye, W.N., Li, Y., Zhang, Y.C., Liu, Z.Y., Song, X.Y., Pei, X.G., Wu, S.F., and Gao, C.F. (2024). Area-wide survey and monitoring of insecticide resistance in the brown planthopper, Nilaparvata lugens (Stål), from 2020 to 2023 in China. Pestic Biochem Physiol *205*, 106173. 10.1016/j.pestbp.2024.106173.

45. Tayler, T.D., Pacheco, D.A., Hergarden, A.C., Murthy, M., and Anderson, D.J. (2012). A neuropeptide circuit that coordinates sperm transfer and copulation duration in Drosophila. Proceedings of the National Academy of Sciences *109*, 20697-20702. 10.1073/pnas.1218246109.

46. Li, H., Cheng, S., Niu, Y., Diao, T., Zhang, Q., and Zhang, W. (2025). A heart releasing neuropeptide that synchronizes brain-heart regulation during courtship behavior. bioRxiv, 2025.2003.2031.646145. 10.1101/2025.03.31.646145.

47. Tayler, T.D., Pacheco, D.A., Hergarden, A.C., Murthy, M., and Anderson, D.J. (2012). A neuropeptide circuit that coordinates sperm transfer and copulation duration in Drosophila. Proceedings of the National Academy of Sciences of the United States of America *109*, 20697-20702. 10.1073/pnas.1218246109.

48. Gospocic, J., Shields, E.J., Glastad, K.M., Lin, Y., Penick, C.A., Yan, H., Mikheyev, A.S., Linksvayer, T.A., Garcia, B.A., Berger, S.L., et al. (2017). The Neuropeptide Corazonin Controls Social Behavior and Caste Identity in Ants. Cell *170*, 748-759.e712. 10.1016/j.cell.2017.07.014.

49. Hou, Q.-L., Chen, E.-H., Jiang, H.-B., Yu, S.-F., Yang, P.-J., Liu, X.-Q., Park, Y., Wang, J.-J., and Smagghe, G. (2018). Corazonin Signaling Is Required in the Male for Sperm Transfer in the Oriental Fruit Fly Bactrocera dorsalis. Front Physiol *9*. 10.3389/fphys.2018.00660.

50. Shohat-Ophir, G., Kaun, K.R., Azanchi, R., Mohammed, H., and Heberlein, U. (2012). Sexual deprivation increases ethanol intake in Drosophila. Science *335*, 1351-1355. 10.1126/science.1215932.

51. Zer-Krispil, S., Zak, H., Shao, L., Ben-Shaanan, S., Tordjman, L., Bentzur, A., Shmueli, A., and Shohat-Ophir, G. (2018). Ejaculation Induced by the Activation of Crz Neurons Is Rewarding to Drosophila Males. Current Biology *28*, 1445-1452.e1443. 10.1016/j.cub.2018.03.039.

52. Cheng, J., Zhao, P., Zhu, L., Zhu, F., Tian, Z., Shen, Z., Liu, X., and Liu, X. (2022). Corazonin signaling modulates the synthetic activity of male accessory gland in Grapholita molesta. Int J Biol Macromol *216*, 446-455. 10.1016/j.ijbiomac.2022.07.025.

53. Yang, C.h., Belawat, P., Hafen, E., Jan, L.Y., and Jan, Y.N. (2008). Drosophila Egg-Laying Site Selection as a System to Study Simple Decision-Making Processes. Science *319*, 1679-1683. 10.1126/science.1151842.

54. Tanaka, Y., Suetsugu, Y., Yamamoto, K., Noda, H., and Shinoda, T. (2014). Transcriptome analysis of neuropeptides and G-protein coupled receptors (GPCRs) for neuropeptides in the brown planthopper Nilaparvata lugens. Peptides *53*, 125-133. 10.1016/j.peptides.2013.07.027.

55. Roller, L., Tanaka, Y., and Tanaka, S. (2003). Corazonin and corazonin-like substances in the central nervous system of the Pterygote and Apterygote insects. Cell Tissue Res *312*, 393-406. 10.1007/s00441-003-0722-4.

56. Nässel, D.R., and Zandawala, M. (2019). Recent advances in neuropeptide signaling in Drosophila, from genes to physiology and behavior. 10.7287/peerj.preprints.27515v2.

57. Kubrak, O.I., Lushchak, O.V., Zandawala, M., and Nässel, D.R. (2016). Systemic corazonin signalling modulates stress responses and metabolism in Drosophila. Open Biol *6*. 10.1098/rsob.160152.

58. Nallasivan, M.P., Singh, D.N.D., Saleh, M.S.R.S., and Soller, M. (2024). Sex-peptide targets distinct higher order processing neurons in the brain to induce the female post-mating response. eLife Sciences Publications, Ltd.

59. Isaac, R.E., Li, C., Leedale, A.E., and Shirras, A.D. (2010). Drosophila male sex peptide inhibits siesta sleep and promotes locomotor activity in the post-mated female. Proc Biol Sci *277*, 65-70. 10.1098/rspb.2009.1236.

60. Bath, E., Bowden, S., Peters, C., Reddy, A., Tobias, J.A., Easton-Calabria, E., Seddon, N., Goodwin, S.F., and Wigby, S. (2017). Sperm and sex peptide stimulate aggression in female Drosophila. Nat Ecol Evol *1*, 0154. 10.1038/s41559-017-0154.

61. Predel, R., Neupert, S., Russell, W.K., Scheibner, O., and Nachman, R.J. (2007). Corazonin in insects. Peptides *28*, 3-10. 10.1016/j.peptides.2006.10.011.

62. Boerjan, B., Verleyen, P., Huybrechts, J., Schoofs, L., and De Loof, A. (2010). In search for a common denominator for the diverse functions of arthropod corazonin: a role in the physiology of stress? Gen Comp Endocrinol *166*, 222-233. 10.1016/j.ygcen.2009.09.004.

63. Veenstra, J.A. (2009). Does corazonin signal nutritional stress in insects? Insect biochemistry and molecular biology *39*, 755-762. 10.1016/j.ibmb.2009.09.008.

64. Zhao, Y., Bretz, C.A., Hawksworth, S.A., Hirsh, J., and Johnson, E.C. (2010). Corazonin neurons function in sexually dimorphic circuitry that shape behavioral responses to stress in Drosophila. Plos One *5*, e9141. 10.1371/journal.pone.0009141.

65. Veenstra, J.A. (1989). Isolation and structure of corazonin, a cardioactive peptide from the American cockroach. Febs Lett *250*, 231-234. 10.1016/0014-5793(89)80727-6.

66. Tawfik, A.I., Tanaka, S., De Loof, A., Schoofs, L., Baggerman, G., Waelkens, E., Derua, R., Milner, Y., Yerushalmi, Y., and Pener, M.P. (1999). Identification of the gregarization-associated dark-pigmentotropin in locusts through an albino mutant. Proceedings of the National Academy of Sciences of the United States of America *96*, 7083-7087. 10.1073/pnas.96.12.7083.

67. Tanaka, Y., Hua, Y., Roller, L., and Tanaka, S. (2002). Corazonin reduces the spinning rate in the silkworm, Bombyx mori. J Insect Physiol *48*, 707-714. 10.1016/s0022-1910(02)00094-x.

68. Kim, Y.J., Spalovská-Valachová, I., Cho, K.H., Zitnanova, I., Park, Y., Adams, M.E., and Zitnan, D. (2004). Corazonin receptor signaling in ecdysis initiation. Proceedings of the National Academy of Sciences of the United States of America *101*, 6704-6709. 10.1073/pnas.0305291101.

69. Imura, E., Shimada-Niwa, Y., Nishimura, T., Hückesfeld, S., Schlegel, P., Ohhara, Y., Kondo, S., Tanimoto, H., Cardona, A., Pankratz, M.J., and Niwa, R. (2020). The Corazonin-PTTH Neuronal Axis Controls Systemic Body Growth by Regulating Basal Ecdysteroid Biosynthesis in Drosophila melanogaster. Current biology : CB *30*, 2156-2165.e2155. 10.1016/j.cub.2020.03.050.

70. Zandawala, M., Nguyen, T., Balanya Segura, M., Johard, H.A.D., Amcoff, M., Wegener, C., Paluzzi, J.P., and Nassel, D.R. (2021). A neuroendocrine pathway modulating osmotic stress in Drosophila. Plos Genet *17*, e1009425. 10.1371/journal.pgen.1009425.

71. Xi, J., Hamanaka, Y., and Shiga, S. (2025). Corazonin mediates photoperiodically induced diapause in the bean bug Riptortus pedestris. J Exp Biol *228*. 10.1242/jeb.250528.

72. Tian, S., Zandawala, M., Beets, I., Baytemur, E., Slade, S.E., Scrivens, J.H., and Elphick, M.R. (2016). Urbilaterian origin of paralogous GnRH and corazonin neuropeptide signalling pathways. Sci Rep *6*, 28788. 10.1038/srep28788.

73. Yañez Guerra, L.A., and Zandawala, M. (2023). Discovery of Paralogous GnRH and Corazonin Signaling Systems in an Invertebrate Chordate. Genome Biol Evol *15*. 10.1093/gbe/evad108.

74. Knobil, E. (1988). The hypothalamic gonadotrophic hormone releasing hormone (GnRH) pulse generator in the rhesus monkey and its neuroendocrine control. Hum Reprod *3*, 29-31. 10.1093/oxfordjournals.humrep.a136647.

75. Millar, R.P. (2005). GnRHs and GnRH receptors. Anim Reprod Sci *88*, 5-28. 10.1016/j.anireprosci.2005.05.032.

76. Bergland, A.O., Chae, H.S., Kim, Y.J., and Tatar, M. (2012). Fine-scale mapping of natural variation in fly fecundity identifies neuronal domain of expression and function of an aquaporin. Plos Genet *8*, e1002631. 10.1371/journal.pgen.1002631.

77. Barredo, C.G., Gil-Marti, B., Deveci, D., Romero, N.M., and Martin, F.A. (2020). Timing the Juvenile-Adult Neurohormonal Transition: Functions and Evolution. Front Endocrinol (Lausanne) *11*, 602285. 10.3389/fendo.2020.602285.

78. McKim, T.H., Gera, J., Gayban, A.J., Reinhard, N., Manoli, G., Hilpert, S., Helfrich-Förster, C., and Zandawala, M. (2024). Synaptic connectome of a neurosecretory network in the Drosophila brain. bioRxiv. 10.1101/2024.08.28.609616.

79. Wu, S.-F., Jv, X.-M., Li, J., Xu, G.-J., Cai, X.-Y., and Gao, C.-F. (2017). Pharmacological characterisation and functional roles for egg-laying of a β-adrenergic-like octopamine receptor in the brown planthopper Nilaparvata lugens. Insect biochemistry and molecular biology *87*, 55-64. https://doi.org/10.1016/j.ibmb.2017.06.008.

80. Krogh, A., Larsson, B., von Heijne, G., and Sonnhammer, E.L. (2001). Predicting transmembrane protein topology with a hidden Markov model: application to complete genomes. J Mol Biol *305*, 567-580. 10.1006/jmbi.2000.4315.

81. Livak, K.J., and Schmittgen, T.D. (2001). Analysis of Relative Gene Expression Data Using Real-Time Quantitative PCR and the 2−ΔΔCT Method. Methods *25*, 402-408. https://doi.org/10.1006/meth.2001.1262.

82. Sun, H., Bu, L.-A., Su, S.-C., Guo, D., Gao, C.-F., and Wu, S.-F. (2023). Knockout of the odorant receptor co-receptor, orco, impairs feeding, mating and egg-laying behavior in the fall armyworm Spodoptera frugiperda. Insect biochemistry and molecular biology *152*. 10.1016/j.ibmb.2022.103889.

83. Zhang, Y.C., Gao, Y., Ye, W.N., Peng, Y.X., Zhu, K.Y., and Gao, C.F. (2023). CRISPR/Cas9-mediated knockout of NlCYP6CS1 gene reveals its role in detoxification of insecticides in Nilaparvata lugens (Hemiptera: Delphacidae). Pest management science *79*, 2239-2246. 10.1002/ps.7404.

84. Yan, H., Opachaloemphan, C., Carmona-Aldana, F., Mancini, G., Mlejnek, J., Descostes, N., Sieriebriennikov, B., Leibholz, A., Zhou, X., Ding, L., et al. (2022). Insulin signaling in the long-lived reproductive caste of ants. Science *377*, 1092-1099. 10.1126/science.abm8767.